Using turbine expanders to recover exothermic reaction heat for the combined production of power and chemicals

by

Jaco Perold

Submitted in fulfilment of part of the requirements for the degree of

Master of Engineering (Chemical Engineering)

in the

Faculty of Engineering, Built Environment and Information Technology

University of Pretoria

October 2001

Using turbine expanders to recover exothermic reaction heat for the combined production of power and chemicals

Author: Jaco Perold
Supervisor: I. L. Greeff
Department: Chemical Engineering
Degree: Master of Engineering (Chemical Engineering)

Synopsis

Many reactions carried out in the chemical industry are exothermic. The heat liberated by the reaction is often transferred to another medium such as steam by heat exchange. This heat can then be used elsewhere or be used to generate power via a steam cycle.

In this work the focus is on another method of reaction heat recovery. When an exothermic reaction is conducted at elevated pressures, a turbine expander can be placed directly behind the reactor. The hot, high-pressure product gas from the reactor can then be expanded in the turbine. During the expansion process the physical energy of the product gas is converted to kinetic energy (or electricity if the turbine is connected to a generator).

Three chemical processes were studied to determine the feasibility of turbine integration into the processes. They are ethylene oxide production, phthalic anhydride production and the hydrodealkylation of alkylaromatic compounds. The chosen processes differ in terms of reactor operation, reactant conversion as well as the presence or absence of recycle loops.

Simulation models were developed for the mentioned processes with the process simulator Aspen Plus®. Results from the simulations show that, without the turbine, the processes require power from external sources. They can however operate independently from external power sources when a turbine is present. Excess power can be exported or used for electricity generation. It is therefore feasible to incorporate turbine expansion units in all the processes considered.

The operating conditions of some unit operations have to be changed to accommodate the turbine expander. With the additional product namely power, a re-evaluation of all the operating conditions and tradeoffs in the process is necessary. Further investigation into the impact of turbine integration on the optimal operating conditions of the process is therefore recommended.

Traditional definitions used to evaluate the performance of a process generating or consuming power, were found to be inadequate for use in processes where power and chemicals are produced together. New performance parameters are required for the evaluation of processes where power and chemicals are produced simultaneously.

An exergy analysis was performed for one of the cases. This analysis method provides insight as to where thermodynamic losses occur in a process. The exergy analysis was useful to quantify the losses occurring in an isenthalpic expansion valve, and the savings obtained by replacing such a valve with an expansion turbine.

Keywords: coproduction, exergy analysis, process integration, energy conversion, turbine expander.

Die gebruik van ontspanningsturbines om eksotermiese reaksiewarmte te herwin vir gesamentlike produksie van krag en chemikalieë

Outeur: Jaco Perold
Studieleier: I. L. Greeff
Departement: Chemiese Ingenieurswese
Graad: Magister in Ingenieurswese (Chemiese Ingenieurswese)

Sinopsis

Heelwat reaksies wat uitgevoer word in die chemiese industrie is eksotermies. Die hitte wat vrygestel word tydens die reaksie word dikwels oorgedra na 'n ander medium soos stoom deur hitteruiling. Die hitte kan dan elders aangewend word of dit kan gebruik word om elektrisiteit op te wek in 'n stoomsiklus.

Die fokus in hierdie werk is egter op 'n ander metode van reaksiewarmte herwinning. Wanneer 'n eksotermiese reaksie plaasvind by hoë druk kan 'n ontspanningsturbine direk na die reaktor geplaas word. Die warm, hoë druk produkgas uit die reaktor kan onstpan word in die turbine. Gedurende die ontspanningsproses word die fisiese energie van die produkgas omgesit na kinetiese energie (of elektrisiteit indien die turbine aan 'n generator gekoppel is).

Drie chemiese prosesse is ondersoek om die uitvoerbaarheid te bepaal van die direkte integrasie van turbines in chemiese prosesse. Die prosesse is etileen oksied- en ftaalsuur anhidried produksie asook die hidrodealkielering van alkielaromatiese verbindings. Die gekose prosesse verskil ten opsigte van die bedryf van die reaktor, omsetting van die reagense en die teenwoordigheid of afwesigheid van hersirkulasiestrome.

Simulasie modelle van die prosesse is ontwikkel met die simulasiepakket Aspen Plus®. Die resultate wys dat krag van eksterne bronne ingevoer moet word om die prosesse sonder die ontspanningsturbines te bedryf. Wanneer turbines teenwoordig is

kan die prosesse bedryf word sonder die eksterne kragbronne. Die oormaat energie wat genereer word kan elders gebruik word of alternatiewelik gebruik word vir elektrisiteitsopwekking. Dit is dus 'n aantreklike opsie om ontspanningsturbines te integreer in al die prosesse wat ondersoek is.

Die bedryfstoestande van sommige eenheidsprosesse moet aangepas word om die ontspanningsturbine te akkommodeer. As gevolg van die addisionele produk, naamlik krag, wat uit die proses verkry word, is dit nodig om die bedryfstoestande en kompromieë tussen parameters in die proses te hersien. Verdere ondersoek is nodig om die impak van ontspanningsturbine integrasie op die optimale bedryfstoestande van 'n proses te bepaal.

Die tradisionele parameters wat gebruik word om die werkverrigting van prosesse wat krag genereer of benodig te evalueer, is nie geskik vir prosesse waar krag en chemiese produkte gesamentlik produseer word nie. Nuwe werkverrigtingsparameters is dus nodig vir die evaluering van prosesse wat beide krag en chemikalieë produseer.

'n Eksergie analise is uitgevoer vir een van die gevallestudies. Die metode van analise leen insig oor waar termodinamiese verliese in die proses plaasvind. Die eksergie analise was nuttig om die verliese in isentalpiese ontspanningskleppe te kwantifiseer, asook om die besparings te bepaal wat behaal kan word deur sulke kleppe met ontspanningsturbines te vervang.

Sleutelwoorde: gekombineerde produksie, eksergie analise, proses integrasie, energie omsetting, ontspanningsturbine.

Acknowledgements

I want to thank:

My heavenly Father without whom I could not have finished this project successfully.

I.L. Greeff for her guidance and supervision.

Iscor for giving me the opportunity to pursue my interest.

My family for their unconditional love and support: my father for persuading me to continue my studies, my mother for her interest, my brother and sister for looking up to me.

Marlize for her patience, encouragement and companionship.

Ir. P. P. A. J. van Schijndel, Dr. ir. K. J. Ptasinski and Prof. dr. ir. F. J. J. G. Janssen for their supervision for the part of the work done at the Technical University of Eindhoven, the Netherlands.

Financial support from the Netherlands Organisation for International Cooperation in Higher Education and the Centre for Environmental Technology at the Technical University of Eindhoven are gratefully acknowledged.

Table of Contents

List of Figures

List of Tables

Nomenclature

Greek Symbols

Δ	Change	-
ε	Specific exergy	kJ/kmol
γ	Activity coefficient	-
η	Efficiency	-
κ	Heat capacity ratio	-
τ	Dimensionless exergetic temperature	-

Alphabetic Symbols

C	Concentration	$kmol/m^3$
C_P	Heat capacity at constant pressure	kJ/kmol.K
C_v	Heat capacity at constant volume	kJ/kmol.K
$\dot{E}$	Exergy	kJ/s
h	Specific enthalpy	kJ/kmol
H	Enthalpy	kJ/s
$\dot{I}$	Irreversibility rate (exergy loss)	kW
$\dot{m}$	Material flow	kg/s or kmol/s
P	Pressure	bar
Q	Heat	kJ/s
r	Reaction rate	$kmol/m^3.s$
R	Universal gas constant	kJ/kmol.K
s	Specific entropy	kJ/kmol.K
T	Temperature	°C or K
W	Work	kJ/kmol
$\dot{W}$	Power	kW or MW
x	Mole fraction	-

Subscripts

0	Chemical exergy or Environmental conditions
1	Initial conditions
2	Final conditions
cold	Low temperature heat transfer (power cycles)
constant	Constant power term in ethylene oxide case study
DOP	Degree of perfection
EO	Ethylene oxide
hot	High temperature heat transfer (power cycles)
k	Kinetic
p	Potential
ph	Physical
pump	Pump (power)
r	System boundary temperature
net	Net (power)
TC	Thermal conversion

Superscripts

0	Standard chemical exergy
Q	Exergy associated with heat transfer

Chapter 1: Introduction

Many reactions carried out in the chemical industry are exothermic in nature. To reduce the operating costs of the process, the heat liberated by the reaction is often transferred to another medium usually steam by heat exchange. This heat can then be used elsewhere or be used to generate power via a steam cycle.

Should the reaction be conducted above atmospheric pressure, another alternative of energy recovery presents itself. An expansion turbine can be placed directly behind the reactor. Hot, high-pressure product gas from the reactor can be expanded in a turbine during which the physical energy of the product gas is converted to kinetic energy (or electricity if the turbine is connected to a generator). Janssen, Verkooijen and Ploumen patented this concept in 1997. For the purposes of this investigation, a turbine such as the one just described, is referred to as a chemoturbine.

The integration of a chemoturbine in a chemical process does however pose new challenges. At times, it requires flowsheet modifications or changes in the operating conditions of the process units. The role of utilities (reactor cooling liquid, electricity and steam etc.) also changes, with the focus on energy recovery and withdrawal now falling on the chemical process fluid itself.

Recently Greeff, Ptasinski and Janssen analysed an ammonia process that includes a chemoturbine (2001). Their results showed that, even without process optimisation, enough energy could be recovered from the chemoturbine to drive the compressor and supply part of the required refrigeration work for separation.

It was therefore decided to extend the concept further by evaluating the feasibility of chemoturbine integration with other chemical processes of industrial importance.

Three chemical processes are studied: ethylene oxide production, phthalic anhydride production and the hydrodealkylation of alkylaromatic compounds. Literature and/or real plant data were used for the development of simulation models with the process simulator Aspen Plus (Aspen). This is followed by an alteration of the model to

accommodate a chemoturbine as well as a comparison of the processes with and without the chemoturbine. An exergy analysis is performed for the phthalic anhydride process to illustrate the usefulness of this method of analysis and the advantages of chemoturbine integration into chemical processes. The exergy calculations were performed with the Exercom software package. Issues such as heat removal from the reactor, reactant conversion and the presence of recycle loops also receive attention.

Chapter 2: Theory and Literature Survey

2.1 Combined Power and Chemical Production

Combined production of heat and power has already matured as a technology for improving the thermodynamical efficiencies of energy conversion systems (Greeff *et al.*, 2001: 2). Modern power plants not only provide electricity to end users, but also supply low-quality heat for domestic heating purposes (Dijkema *et al.*, 1998: 115).

However, due to the traditional approach of producing chemicals and power separately, the possibility of co-producing chemicals and power has not achieved the same level of maturity (Greeff *et al.*, 2001: 2). Nevertheless, some processes have been proposed for combined chemicals and power production. These include:

- combining gas turbine cycles with steam methane reforming (Harvey & Kane, 1997) and methanol synthesis (Stahl, 1983; Scharpf & Sorensen, 1997),
- using gas turbine exhaust gases as an oxygen source in cracking furnaces (Dijkema, Luteijn & Weijnen, 1998: 118),
- integrating fuel cells in methanol synthesis plants (Dijkema *et al.*, 1998: 123) and
- the coupling of a zero emission turbine with reversible chemical reactions (Prokopiev, Aristov & Parmon, 1997).

As expected, there are various degrees of combining power and chemical production. It ranges from the inclusion of a single energy conversion unit such as a steam boiler, expansion turbine or cracking furnace (Dijkema *et al.*, 1998: 113) to the complete integration of power and chemical plants capable of supplying large amounts of chemical products and electrical power.

When a steam boiler or furnace is integrated into a chemical plant, energy has to be transferred between the chemical process fluids and the steam boiler or furnace fluids in the form of heat because the fluids are not in direct contact with each other (Dijkema *et al.*, 1998: 113). To minimise the heat exchanger area (and cost), considerable temperature driving forces are used to transfer energy between these

fluids. Unfortunately, large thermodynamical losses occur as a result of this temperature difference (Kotas, 1995: 121) and hence it is not the best available method for energy transfer.

An expansion turbine is an alternative energy conversion unit that does not involve heat exchange between two fluids. The turbine can be placed directly in the chemical process and recover energy from the process fluids as kinetic energy (Janssen, Verkooijen & Ploumen, 1997: 2). A number of patents on the integration of turbines in process streams have been granted and are reviewed in the next section.

2.2 Patent Review of Chemical Processes with Integrated Turbine Devices

Janssen *et al.* (1997) patented a concept capable of delivering both a chemical product and power from an exothermic reaction conducted at high pressure. Reactants are compressed to the reactor pressure where they react under adiabatic conditions. Since no heat removal is permitted, heat liberated in the reaction causes a rise in the internal energy of the reaction mixture and a temperature increase is observed towards the reactor outlet. The resulting gas mixture is expanded in a turbine placed directly after the reactor. Upon expansion, the internal energy of the gas is converted to kinetic energy. The latter can be employed to fulfil process compression requirements and/or be used to generate electricity. This process operates as an open cycle.

Of particular advantage in this concept is that the physical energy of the reactor product is converted to power in the expansion process (Janssen *et al.*, 1997). No heat exchange to a power cycle fluid is required before reaction heat recovery occurs. By eliminating the heat exchanger, the thermodynamical losses associated with heat transfer are also avoided.

In 1981, Barber, Muenger and Alexander invented a process that combines a chemical production plant with a Brayton cycle. In this combination, moderate temperature heat, recovered from the exothermic reaction, is used to preheat the working fluid for the Brayton cycle. By doing so, the amount of high temperature heat required for

power production is reduced. In turn, the Brayton cycle delivers a substantial amount of the compression requirements for the reactor feed.

As in the patent by Janssen *et al.*, (1997), the chemical and power sections share a common working fluid. The unreacted recycle gases are employed as the working fluid in the Brayton cycle. However in the Barber *et al.* patent, heat is still exchanged between the process streams: the hot turbine exhaust gases are used to preheat the reactor feed and the reactor product gases are used to heat recycle gases prior to entering the Brayton cycle turbine. With all this heat exchange, the thermodynamical losses associated with heat transfer have not been avoided.

A patent from 1967, granted to Horton, shows how high temperature reaction heat, liberated from a reaction conducted at low pressure, can be transferred to a stream at high pressure and low temperature before the latter is expanded. This is the case in a two-step nitric acid production process where the oxidation of ammonia (reaction 1) is followed by the absorption of nitric oxide in water (reaction 2):

$$4NH_3 + 5O_2 \Leftrightarrow 4NO + 6H_2O \quad (1)$$

$$2H_2O + 3O_2 + 4NO \Leftrightarrow 4HNO_3 \quad (2)$$

The first reaction is carried out at temperatures between 700 and 1000°C, but, for thermodynamical reasons, the pressures are kept low (1-3 bar). The second reaction takes place in an absorption column at low temperatures (about 25°C) but at pressures from 4 to 8 bar (Horton, 1969). Horton suggests that energy recovery takes place by tail gas expansion alone instead of the typical energy recovery system comprising of a waste heat boiler and tail-gas expander. No steam is raised

Horton's invention has several advantages: energy recovery is better than in conventional nitric acid plants, absorption can be carried out at the more favourable, higher pressures without having to import power from and external source. The overall plant layout is also simplified by the omission of the waste heat boiler (Horton, 1969:3). In spite of these advantages, the thermodynamical losses associated

with heat exchange between the hot product from the oxidation reactor and the tail gases, are still present.

Linnhoff, Le Leur and Pretty (1988) also patented a concept wherein expansion does not take place directly after the reactor. They suggest that a feed stream, exceeding the full load capacity of the reactor system, be compressed. The excess of high-pressure feed gas bypasses the reactor system. It is heated with high temperature heat removed from the reactor and is expanded with the reactor products in a turbine expander. This concept can be applied to any exothermic, high-pressure reaction, but works particularly well with air based reactions such as the oxidation of ammonia (in nitric acid production) and the oxidation of sulphur (in sulphuric acid production) as air can be used as the additional gas to be compressed.

An important benefit of the Linnhoff *et al.* patent is that the work generated in the expansion process is less sensitive to load changes in the reaction system. A relatively steady amount of power is provided without sacrificing flexibility in chemical production rate. On a negative note, a lot of heat exchange still takes place that brings about unnecessary thermodynamical losses.

2.3 Exergy Analysis

For a long time, the use of engineering thermodynamics was limited to evaluation of process effectiveness by means of the First law of Thermodynamics. Energy balances were used to determine the "unaccounted for" heat transfer between systems and the environment, and performance criteria such as thermal efficiencies were calculated to evaluate process operation (Kotas, 1995: xix).

During this time, process performance was evaluated with the First law of Thermodynamics, the energy balance, without ever evaluating its suitability for this type of analysis. Indeed, when the suitability of the energy balance is assessed, several shortcomings can be identified.

In an energy balance, all forms of energy (ordered, disordered, thermal, chemical, mechanical etc.) are treated as equivalent without differentiating between the various

qualities of energy crossing the system boundary (Kotas, 1995: xix). Hence, 100 kilojoules of work will be treated in the same way as 100 kilojoules of low-grade energy rejected from the condenser of a steam cycle.

As differences in energy quality are ignored, changes in energy quality are not visible and internal process losses (due to the thermodynamic imperfection of the process itself) do not receive any attention.

The Second law of Thermodynamics governs the limits of convertibility between the different energy forms (Kotas, 1995: xx) and hence the quality of energy forms. It should form the basis for the thermodynamical analysis of processes, but with abstract concepts such as entropy, its use is not widespread.

Exergy analysis is a relatively new technique that combines the energy balance (First law) with the entropy production rate (Second law). Through this combination, it is not necessary to use the Second law explicitly (Kotas, 1995: xx). The power of this analysis lies in its ability to point out the decline in energy quality in energy intensive processes. This leads to a better understanding of the influences of the thermodynamic phenomena on the process.

The name of the analysis method is derived from the universal standard of energy quality used to account for the variable qualities of energy forms (Kotas, 1995: 32). This standard is called exergy. As all forms of energy can be converted to work, exergy is defined as the maximum work that can be obtained from a given form of energy when it is brought to a state of thermodynamic equilibrium with the components in the natural environment (or dead state) by means of reversible processes. The only interaction allowed in these reversible processes is with the abovementioned components in nature (Szargut, Morris & Steward, 1988: 7).

An exergy balance is similar to an energy balance, but instead of being based on a conservation law, it is based on a law of degradation (Kotas, 1995: 32). For a steady state flow system such as a chemical process the exergy balance is (Kotas, 1995: 63):

$$\sum_{in} \dot{E} + \dot{E}^{Q} + \dot{W} = \sum_{out} \dot{E} + \dot{I} \qquad (3)$$

The first four terms refer to the exergy associated with the three possible types of energy transfer over the system boundaries:

- exergy associated with material flow ($\dot{E}$)
- exergy associated with heat transfer ($\dot{E}^{Q}$)
- exergy associated with work transfer ($\dot{W}$)

and $\dot{I}$ is the irreversibility rate or exergy loss due to the thermodynamic imperfection of the system under consideration. Each term is discussed shortly in Appendix A. For more information, consult textbooks on exergy analysis by Kotas (1995) and Szargut *et al.* (1998).

Exergy calculations involve a large amount of thermodynamic parameters. Even in the analysis of straightforward processes, the calculations can become too cumbersome to perform by hand, making computer calculations a necessity. Several workers have written subroutines to perform exergy calculations in Aspen Plus (Bram & de Ruyck, 1997; Rosen, 1996), but these were written as research tools and were not released commercially.

One software package that has been released commercially is Exercom. It works as an add-on package to Aspen Plus and calculates the exergy associated with material streams (Hinderink *et al.*, 1996).

Results of exergy calculations can be reported in several ways. Among the most commonly used, include second law efficiencies and irreversibility rates. As with first law efficiency definitions, there are many exergy efficiency definitions to characterise a system's thermodynamic perfection. A number of efficiency definitions were reviewed by Sorin, Lambert and Paris (1998). The degree of perfection (DOP), as described in Szargut *et al.* (1988: 19), is a very popular efficiency definition:

$$\eta_{DOP} = \frac{\text{Exergy of useful products}}{\text{Exergy input}} \qquad (4)$$

According to Tsatsaronis (1999: 96), exergy efficiencies should only be used to compare similar processes operating under similar conditions. Comparison of different components should occur based on the irreversibility rate in each unit.

As a final point, it is important to realise that exergy analysis has shortcomings too. An exergy analysis does not make detailed recommendations for improvements. It only indicates where the process can be improved and hence, which areas should be looked at more closely (Szargut *et al.*, 1988: 2). Secondly, it cannot state whether a possible improvement is practicable. This has to be determined by an economic analysis (Szargut *et al.*, 1998: 3).

Chapter 3: Ethylene Oxide Production

3.1 Introduction

The production process of ethylene oxide (EO) involves a typical flowsheet of a chemical process with reaction, separation and recycle steps.

As ethylene oxide is produced by a partial oxidation reaction, it is highly exothermic. This process is interesting because a portion of the reaction heat is absorbed by the reaction mixture (in the form of a temperature increase) whilst the balance is removed by a coolant. Furthermore, the low per-pass conversion of ethylene makes it an ideal process to study the effect of expansion, separation and recompression on the net power from the recycle loop.

Two flowsheets are developed in Aspen: one without and one with a chemoturbine. These are compared with each other. A sensitivity analysis is performed to investigate the effect of expansion, separation and recompression on the net power from the recycle loop. This is done by varying the chemoturbine outlet pressure.

3.2 The Reaction

Since ethylene oxide's discovery in 1863, many have tried to produce it by the direct oxidation of ethylene with oxygen but to no avail. Success came in 1931 when Lefort discovered that metallic silver catalyses the partial oxidation of ethylene according to the reaction (Rebsdat & Mayer, 1991: 121):

$$2C_2H_4 + O_2 \rightarrow 2C_2H_4O \qquad (5)$$

Carbon dioxide and water are the only significant by-products observed in the process. They form by the complete combustion of ethylene:

$$C_2H_4 + 3O_2 \rightarrow 2CO_2 + 2H_2O \qquad (6)$$

and the further oxidation of ethylene oxide (Dever *et al.*, 1995: 925):

$$C_2H_4O + 2.5O_2 \rightarrow 2CO_2 + 2H_2O \quad (7)$$

Reaction 7 is merely reaction 5 subtracted from reaction 6 and hence not an independent reaction. It will not be considered further. Reactions 5 and 6 are exothermic with reaction heats of –107 and –1 323 kJ/mol respectively at 250°C and 15 bar (Rebsdat & Mayer, 1991: 122). Typical reaction conditions are temperatures of 200 to 300°C and pressures of 10 to 30 bar (Rebsdat & Mayer, 1991: 122).

Selectivity and conversion have an inverse relationship with maximum selectivity reached at minimum conversion. Practical conversion values are chosen to achieve ethylene oxide concentrations of 1-2 vol% at the reactor outlet. As a result the ethylene conversion is typically 7-15% (Rebsdat & Mayer, 1991: 124-125).

3.3 The Production Process

Prior to Lefort's discovery, ethylene oxide was produced by the chlorohydrin process. Today the silver-catalysed partial oxidation process is used exclusively (Rebsdat & Mayer, 1991: 120; Dever *et al.*, 1995: 925).

Two process variations exist based on the source of oxygen: air and pure oxygen. As the majority of ethylene oxide is produced in oxygen-based processes (Rebsdat & Mayer, 1991: 123) this type will be considered further. A flowsheet of an oxygen-based process is shown in Figure 1.

Make-up oxygen and ethylene are mixed and compressed to the reactor pressure. After compression it mixes with a high-pressure recycle stream containing mostly unreacted ethylene and methane. It is preheated with the reaction product before it enters the reactor.

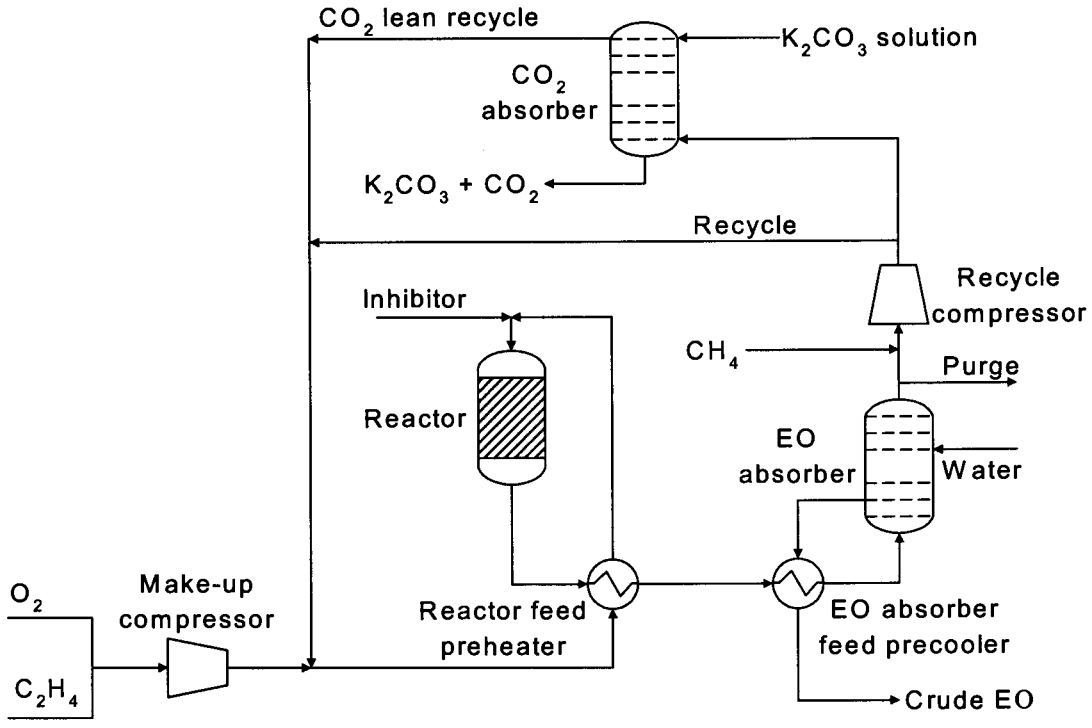

Figure 1: Oxygen-based process for the production of ethylene oxide (adapted from Rebsdat & Mayer, 1991: 123)

The production of ethylene oxide takes place in a packed bed multitubular reactor. It is of the shell and tube type and is comprised of several thousands of reactor tubes (Dever *et al.*, 1995: 926). Vapour phase oxidation inhibitors such as ethylene dichloride or vinyl chloride are usually added at the reactor inlet in parts-per-million quantities to retard the formation of carbon dioxide (Dever *et al.*, 1995: 928).

Even though a part of the reaction heat is absorbed in the form of a temperature increase, the reactor still requires cooling to prevent "hot spots" and runaway conditions. Two possible heat extraction systems exist: evaporation or circulation of the coolant. Evaporative cooling extracts heat more efficiently than circulation cooling, but there are smaller axial temperature differences (i.e. it behaves more like an isothermal reactor). With circulation cooling, a temperature increase towards the reactor outlet is allowed to compensate for the lower reactant concentrations that may otherwise lead to uneconomically low conversions (Rebsdat & Mayer, 1991: 125). In both cases, the coolant may be water or a high-boiling hydrocarbon.

The cooled reaction mixture is sent to two successive absorbers. In the first, virtually all of the ethylene oxide and small amounts of the other reaction species (CO_2, N_2, CH_4, ethylene and aldehydes) dissolve in water (Rebsdat & Mayer, 1991: 124). Absorption takes place at temperatures ranging from 15 to 50°C and pressures from 7 to 20 bar (Cunningham, Foster & Vanderwater, 1971: 6). The crude ethylene oxide stream flows to an ethylene oxide desorber and distillation column (not shown) before the final product is recovered whilst the gaseous recycle stream proceeds in the direction of the second absorber.

A small portion of the gas from the first absorber is purged to prevent the accumulation of inert compounds in the system. Methane is added next as a diluent gas. Its main function is to raise the flammable limit and reduce the peak temperature difference in the reactor bed (Dever *et al.*, 1995: 935). The position where methane is introduced to the system does not appear to be fixed as two variations were found in literature (Coombs, Kim & Palombo, 1997; Rebsdat & Mayer, 1991: 123).

Subsequent to the addition of methane, the recycle stream is recompressed because high pressures favour the recovery of CO_2 in the next unit, the CO_2 absorber (Dever *et al.*, 1995: 935). A bypass around the absorber can be used to minimise the size (and cost) of this unit if the CO_2 concentration in the reactor feed can be kept below 15%. This CO_2 concentration limit is necessary as it influences the catalyst activity at high concentrations (Dever *et al.*, 1995: 931).

A hot potassium carbonate solution is used to remove the CO_2 from the recycle gases (Rebsdat & Mayer, 1991: 123). Common operating conditions for CO_2 absorbers are 250°C and 40 bar (Underwood, Dawson & Barney, 1997). The CO_2-lean product from the CO_2 absorber is mixed with the bypass stream before it rejoins fresh feed and repeats the cycle.

3.4 Flowsheet Development and Modelling

3.4.1 Assumptions and Constraints

All the thermodynamic variables were calculated using the Soave Redlich Kwong property method. This decision was primarily based on the high pressures (as mentioned in sections 3.2 and 3.3) that exist in the process. Furthermore, this method is recommended for hydrocarbon processing applications (AspenTech, 1999: 3-38).

All process units were assumed to be well isolated so no heat is lost to the environment. Pressure drop in the reactor, mixer, heat exchanger and absorber units were considered negligible.

To avoid potential convergence problems due to low component flows, the oxidation inhibitors usually added to the reactor inlet (to retard the carbon dioxide formation) were omitted from the model.

3.4.2 Process without a Chemoturbine (Case A)

The oxygen-based ethylene oxide production process was modelled under steady state conditions using Aspen. The process flowsheet is shown in Figure 2.

In the remainder of this section, the various process units and numerical methods used to develop the simulation model are described.

Make-up stream preparation

To protect the catalyst against poisoning, raw materials used in ethylene oxide production have high purity requirements. The make-up stream specifications shown in Figure 3 were used in the simulations and were obtained from literature (Dever *et al.*, 1995: 935-936).

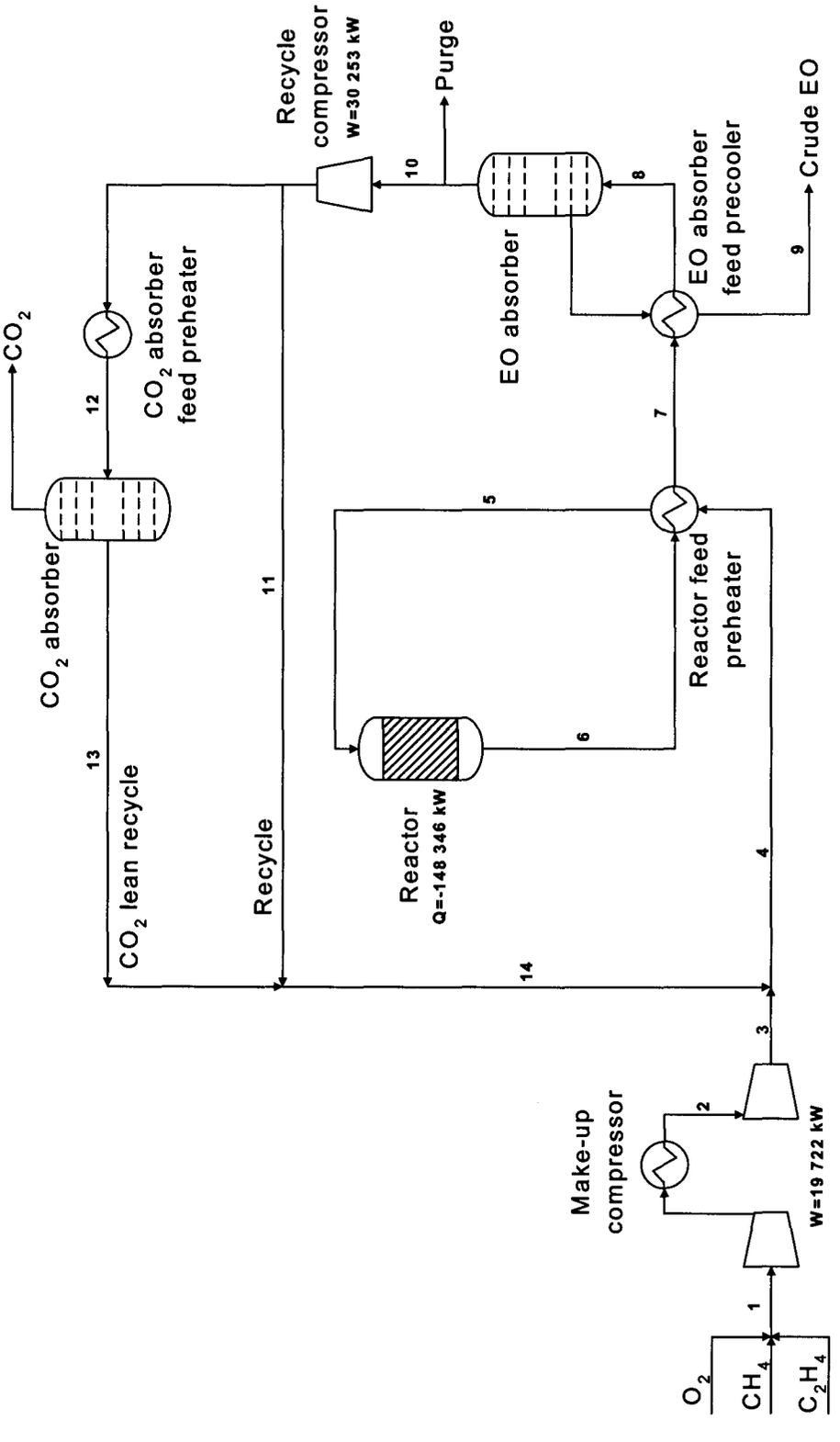

Stream number	1	2	3	4	5	6	7	8	9	10	11	12	13	14
Temperature (°C)	25	50	121	147	200	300	253	25	25	25	90	250	250	155
Pressure (Bar)	1	10	20	20	20	20	20	20	20	20	40	40	40	40
Mole Flow (kmol/h)	5 485	5 485	5 485	49 661	49 661	49 333	49 333	49 333	4 103	45 231	27 084	18 056	17 092	44 176
Mass Flow (ton/h)	146.3	146.3	146.3	1 133.5	1 133.5	1 133.5	1 133.5	1 133.5	101.8	1 031.7	617.8	411.9	369.4	987.2

Figure 2: Flowsheet of ethylene oxide process as simulated in Aspen Plus

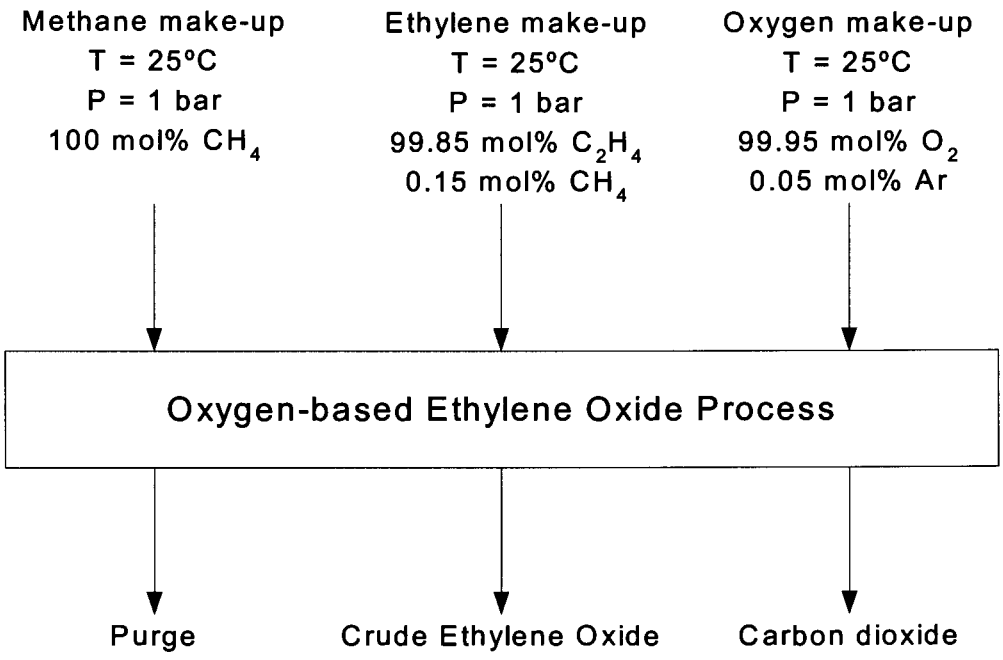

Figure 3: Feed and product streams for the ethylene oxide simulations

An Aspen design specification (numerical solver) was used to adjust the oxygen make-up flow rate to maintain a 6±1% oxygen mole fraction in the reactor feed. This value agrees with the typical mole fraction of oxygen in ethylene oxide reactor feeds (Rebsdat & Mayer, 1991: 124).

Similarly, a second design specification was used to maintain a 50±1% mole fraction of methane in the reactor feed. The manipulated variable was the methane make-up flow rate. Normal methane values found in industrial conditions vary between 1 and 60 mol% (Rebsdat & Mayer, 1991: 124). Besides its diluent function, as described in section 3.3, the methane now has an additional role. It acts as a carrier for the reaction heat and increases the flow through the chemoturbine. The higher flow rate through the chemoturbine increases its power production capacity (see Appendix B for the principle equations governing expansion and compression processes).

Make-up compressor

The mixed make-up stream is compressed in a two-stage compressor with intermediate cooling. The first stage compression is to 10 bar; whereafter the gas is

cooled to 50°C, and compressed in the second stage to the reactor pressure of 20 bar. As a first estimate of compressor efficiency, Aspen's default isentropic efficiency of 72% was used for both stages.

Reactor feed preheater

The hot reactor effluent is used to preheat the feed to the inlet temperature of 200°C.

Reactor

The reactor was modelled using a plug flow reactor model. Reaction kinetics were obtained from Westerterp & Ptasinski (1984: 245-246). These are first-order in oxygen concentration and give the reaction rate per unit mass of catalyst (kmol/s per kg catalyst). For use in the power law kinetic model, the equations had to be rewritten per unit of reactor volume (kmol/s per m^3 reactor volume). The rewritten rate equations are:

$$r_{EO} = 6.0e^{\frac{-59860.8}{RT}} C_{O_2} \qquad (8)$$

for the formation of ethylene oxide according to reaction 5 and

$$r_{CO_2} = 4.2\times10^7 e^{\frac{-89791.2}{RT}} C_{O_2} \qquad (9)$$

for the complete oxidation of ethylene according to reaction 6. The activation energies are in kJ/kmol and the concentrations in kmol/m^3.

A tube diameter of 40mm was used which falls in the range of 20-50mm commonly used in such plants (Rebsdat & Mayer, 1991: 124). The number of tubes, 10 000, was also obtained from literature (Ozero & Landau, 1984: 294). A design specification was used to vary the tube lengths between the typical values of 6 and 12m (Rebsdat & Mayer, 1991: 124) to obtain an ethylene oxide mole fraction of 1.5±0.5%, consistent with literature values (Rebsdat & Mayer, 1991: 124), at the reactor outlet.

With an equal ethylene oxide production rate, comparisons between the processes with and without the chemoturbine can be made with ease. Hence, a fixed ethylene oxide production rate of 655±1 kmol/h was specified for the reactor. Another design specification was used to achieve this by varying the flow rate of the ethylene make-up. Nowadays plants capacities exceed 250 000 tonnes/year or 647 kmol/h (Dever *et al.*, 1995: 927), so this is a realistic specification.

It is well known that ethylene oxide reactors require cooling to prevent reaction runaway (Westerterp & Ptasinski, 1984). As a simplification of an already complex reactor model, no cooling fluid, heat transfer coefficients or the like were specified. A linear temperature increase from 200 to 300°C along the length of the reactor was specified instead. With both a temperature increase and cooling, this reactor has aspects of adiabatic and isothermal operation.

The steam generated by the removal of reaction heat is used to generate additional power via a Rankine-type steam cycle (as reviewed in Appendix C). If a temperature driving force of 20°C is applied, the generated steam will have a temperature of 280°C and the efficiency of the steam cycle will be relatively low. A conservative assumption of 20% heat-to-power-conversion was made to estimate the power generated by the steam cycle.

Ethylene oxide absorber precooler

Even after being used to preheat the reactor feed, the temperature of the reactor product is still above the optimum for ethylene oxide absorption (15-50°C; Cunningham *et al.*, 1971: 6). Further cooling to the chosen temperature of 25°C takes place in the absorber feed precooler.

Ethylene oxide absorber

In section 3.3, the pressure range for ethylene oxide absorption was mentioned as 7 to 20 bar. The high-pressure limit (20 bar) was used in the model as higher pressures increase the absorption efficiency (Dever *et al.*, 1995: 935).

An Aspen RADFRAC model was used to model the absorber. Comparisons of experimental results and data regression analysis revealed the NRTL property method to be suitable for modelling the absorption of ethylene oxide in water (Mistry, King & Paxton, 1997). The flowsheet must be divided into subsections to use multiple property methods. In this case, one flowsheet subsection is required for the Soave Redlich Kwong method and another for the NRTL method. A fifth design specification is also required to calculate the flow rate of the water to the absorber. The additional computations from the new property method and design specification influenced the numerical stability of the system to such an extent that convergence could not be achieved. Consequently an alternative approach had to be used.

It was decided to model the absorber as a black box separator and specify the separation parameters for it. In literature it is mentioned that almost all the ethylene oxide and only small quantities of the other constituents dissolve in water (Rebsdat & Mayer, 1991: 124), therefore the separation parameters shown in Table 1, were used.

Table 1: Separation parameters for ethylene oxide absorber

Species	Mole fraction of feed dissolved in water
Oxygen	0
Ethylene	0.05
Methane	0.05
Ethylene oxide	1
Carbon dioxide	0.05
Water	1
Argon	0

The outlet streams from the absorber were allowed to flash. By doing so, the phases of the outlet streams can be specified. The recycle stream is a vapour and the crude ethylene oxide product is in the liquid phase.

Purge

A small percentage, commonly 0.1-0.2%, of the recycle gas leaving the ethylene oxide absorber is continuously purged to prevent the buildup of inert compounds such

as argon (Rebsdat & Mayer, 1991: 124). In this simulation, a purge fraction of 0.2% was used.

Recycle compressor

Since the second absorber operates at a pressure higher than the first (40 bar), additional compression is required. The recycle compressor increases the pressure to 40 bar at an efficiency of 72% with respect to isentropic operation. This efficiency is the default isentropic efficiency used by Aspen.

Carbon dioxide absorber bypass

As mentioned in section 3.3, not all of the recycle gases have to be treated in the CO_2 absorber. Common concentrations of carbon dioxide in the reactor feed are between 5 and 15% (Rebsdat & Mayer, 1991: 124). At a bypass fraction of 60%, the reactor feed contained five percent CO_2.

Carbon dioxide absorber feed preheater

This feed preheater increases the temperature of the stream to be treated to 250°C, the common temperature for the removal of CO_2.

Carbon dioxide absorber

This absorber was also modelled with a black box separator. A separation efficiency of 90% was assumed. As with the ethylene oxide absorber, the outlet streams were flashed in order to specify their respective phases. The CO_2-lean recycle stream is in the vapour phase whilst the CO_2-rich stream is a liquid.

3.4.3 Process with a Chemoturbine (Case B)

As power generation in turbines are favoured by high inlet temperatures and high pressure ratios (see Appendix B), the best position in a process for a chemoturbine would be at the combination of high pressure and temperature that would render the most power when expansion takes place. The pressure and temperature at the outlet of

the chemoturbine should also be compatible with the requirements of the downstream unit operations.

In the ethylene oxide process, the highest pressure and temperature do not coincide. Conditions at the reactor outlet are 300°C and 20 bar whilst the carbon dioxide absorber operates at 250°C and 40 bar.

The operating pressure of the reactor was increased to 40 bar to coincide with that of the carbon dioxide absorber. This modification is necessary to accommodate the insertion of the chemoturbine directly behind the reactor as shown in Figure 4. As a result of this modification, there are only two pressure levels in the recycle loop of the process. The reactor and carbon dioxide absorber units are on the high-pressure side and the ethylene oxide absorber is on the low-pressure side. Such a scheme corresponds more closely to a Rankine-type power cycle where the pressure ratio for the compressor and turbine are equal. The problem of mixing the high-pressure recycle (40 bar) with the low pressure make-up feed (20 bar) has also been solved.

The reactor pressure of 40 bar is uncommon but there are benefits to it. The increase in pressure will increase the concentrations of the reactants, which in turn increases the reaction rates (Dever *et al.*, 1995: 935). As the reactions take place faster, the reactor length can be shortened to achieve the same conversion. This partially counteracts the increased equipment cost due to the higher pressures.

Changes in the process units necessary to bring about the higher reactor pressure and accommodate the inclusion of the chemoturbine are discussed next.

Make-up compressor

The make-up feed has to be compressed to the higher reactor pressure. The first stage pressure and intercooling temperature were left unchanged at 10 bar and 50°C respectively, but the second stage's outlet pressure was increased to 40 bar. No changes were made to the isentropic efficiencies for the compression stages.

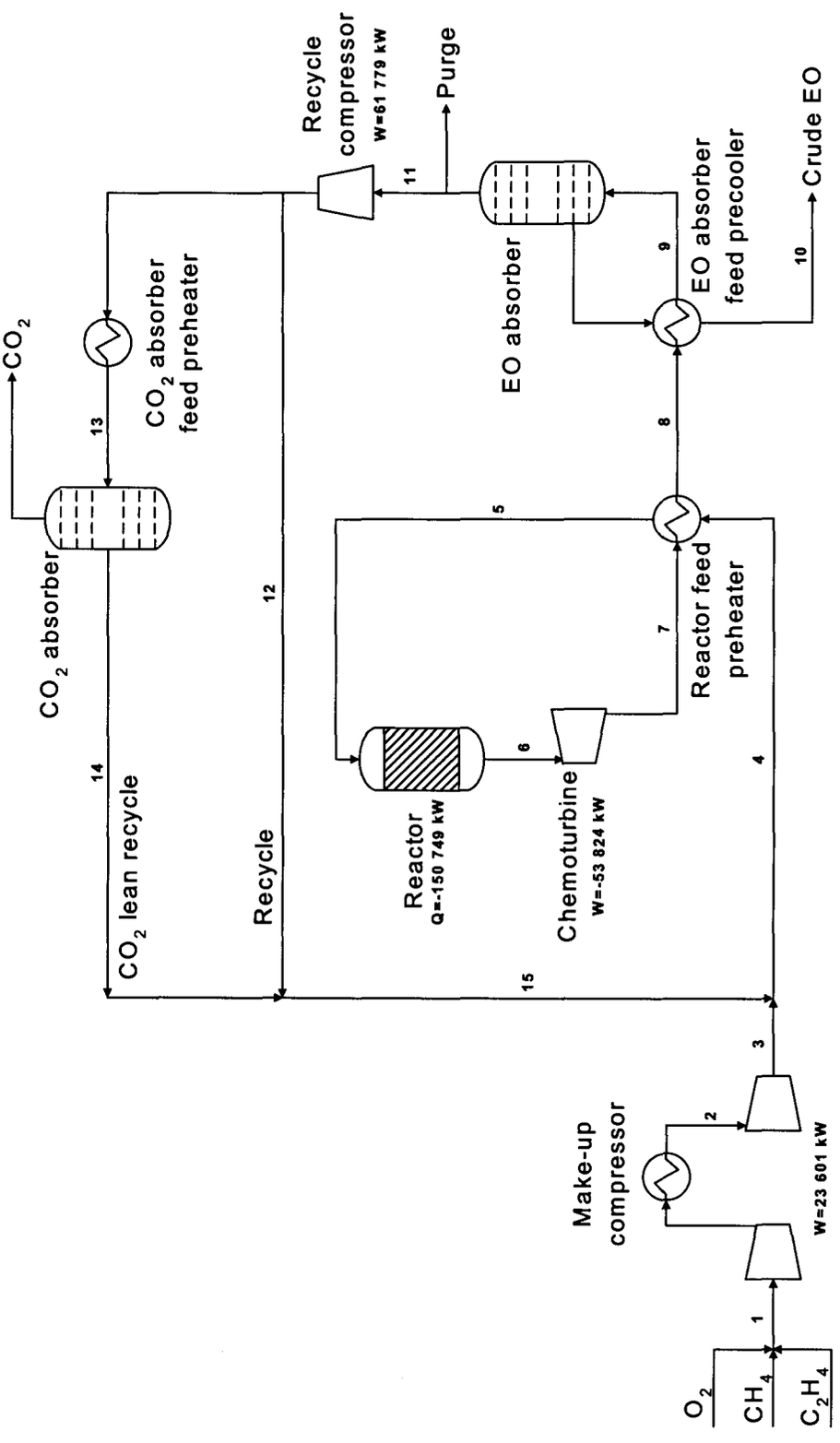

Stream number	1	2	3	4	5	6	7	8	9	10	11	12	13	14	15
Temperature (°C)	25	50	197	194	200	300	219	212	25	25	25	156	250	250	194
Pressure (Bar)	1	10	40	40	40	40	10	10	10	10	10	40	40	40	40
Mole Flow (kmol/h)	5 263	5 263	5 263	45 781	45 781	45 454	45 454	45 454	45 454	3 902	41 469	24 882	16 588	15 637	40 519
Mass Flow (ton/h)	141.1	141.1	141.1	1 045.3	1 045.3	1 045.3	1 045.3	1 045.3	1 045.3	97.3	946.1	567.6	378.4	336.6	904.2

Figure 4: Flowsheet of the ethylene oxide process with chemoturbine as simulated in Aspen Plus

Chemoturbine

A chemoturbine was inserted directly after the reactor. Its outlet pressure, 10 bar, was chosen to coincide with the typical pressures used for the absorption of ethylene oxide (7 to 20 bar). This gives a pressure drop of 30 bar over the chemoturbine. The default isentropic efficiency of 72% was used.

Ethylene oxide absorber

The ethylene oxide absorber in Case A operates at the high-pressure limit of 20 bar for reasons already mentioned. For case B, the lower absorption pressure of 10 bar is expected to be more favourable because more power can be extracted by the chemoturbine. Furthermore, as separation takes place before recompression, the volume to be recompressed is smaller than that expanded. This should contribute favourably to a net power generation.

3.5 Comparison of Case A and Case B

As mentioned in section 3.4.2, Aspen design specifications were used to obtain equal ethylene oxide production rates to facilitate comparisons between the two described cases. These production rates are shown in Table 2 along with other parameters used to evaluate reactor performance.

Table 2: Comparison of reactor performance

Parameter	Case A	Case B
Ethylene conversion	6.0%	6.5%
Selectivity (mol C_2H_4O formed/mol CO_2 formed)	59%	60%
Ethylene oxide production rate (kmol/h)	654.7	654.0

The ethylene conversion and selectivity values are slightly higher for Case B due to the higher reaction pressure. The difference in ethylene oxide production rates is only 0.1%, so the processes can be compared on an absolute basis.

From the stream tables in Figure 2 and Figure 4 (sections 3.4.2 and 3.4.3), one can see that there is an 8% reduction in the recycle flow rates for Case B. The make-up and

product flow rates are 4% lower than that of Case A. The heat exchanger duties shown in Table 3 are also smaller for Case B due to the reduced flow rates.

Table 3: Comparison of heat exchanger duties

Heat exchanger	Case A	Case B	% Reduction
Feed compressor intercooler (kW)	-14 385	-13 815	4%
Ethylene oxide absorber precooler (kW)	-163 720	-121 150	26%
Carbon dioxide absorber preheater (kW)	41 230	22 930	44%

Whereas the heat exchanger duties showed a reduction, the compressor power requirements, shown in Table 4, are considerably higher due to the higher reactor pressure used in Case B.

Table 4: Comparison of compressor and expansion power

	Case A	Case B	% Change
Compression power			
Make-up feed compressor (kW)	19 720	23 600	+16%
Recycle compressor (kW)	30 250	61 780	+51%
Total power required (kW)	49 970	85 380	+41%
Expansion power			
Chemoturbine (kW)	-	-53 820	-
Steam cycle @ 20% heat-to-power conversion (kW)	-29 670	-30 150	+2%
Total power generated (kW)	-29 670	-83 970	+65%
Net power required by the process (kW)	20 300	1 400	-93%
Chemoturbine power/recycle compressor power	-	87%	-

With the introduction of the chemoturbine, the increase in the power generated is greater than the increase in power requirement. Consequently, the process' net power requirement also decreases. This decrease of 93% means that the process can nearly operate independently from external power supplies.

3.6 Sensitivity Analysis

With the ratio of chemoturbine power to recycle compressor power being 87% (Table 4) and the fact that separation occurs between expansion and recompression, it is likely that a range of operating conditions exist where the power produced by the chemoturbine can equal or surpass the amount required by the recycle compressor.

A sensitivity analysis was performed to determine if this is indeed true. Case B was used as the base case. The chemoturbine's outlet pressure was varied within the range of acceptable ethylene oxide absorber pressures (10 to 20 bar), which corresponds to pressure ratios (outlet pressure/inlet pressure) ranging from 0.25 to 0.5. The results are shown in Figure 5.

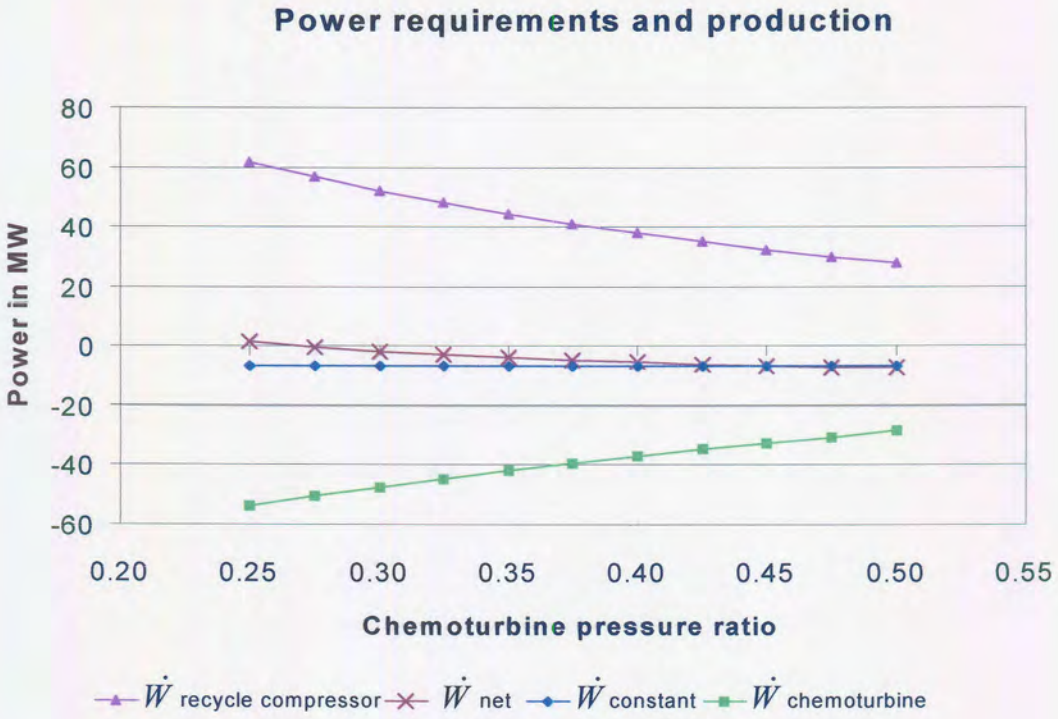

Figure 5: Power requirements and production as functions of the chemoturbine pressure ratio

Curves for the recycle compressor power, chemoturbine power and process net power ($\dot{W}_{net}$) are shown in Figure 5 along with a new term: the constant power ($\dot{W}_{constant}$). The power values of the make-up compressor and steam cycle did not change

significantly compared to that of the recycle compressor and chemoturbine. Their respective values are added and displayed separately as $\dot{W}_{constant}$.

The constant power curve shows that the steam cycle produces more power than that consumed by the make-up feed compressor over the pressure ratio range considered, hence the negative values.

The net power curve is positive for a pressure ratio of 0.25 confirming that Case B requires power from an external source. At a pressure ratio of 0.275, the process becomes independent from external power sources and at even higher pressure ratios, power can be exported from the process.

Even though power can be exported from the process for all pressure ratios larger than 0.275, it does not necessarily mean that the chemoturbine produces enough power to drive the recycle compressor by itself. This is only true for pressure ratios larger than 0.45 where the constant power and net power curves coincide.

Hence, the chemoturbine can supply the total amount of power required by the recycle compressor if its outlet pressure is 18 bar or higher. When this is the case, the net power export from the process is the difference between the steam cycle and make-up compressor power. The maximum amount of power available for export is 7.2 MW and is obtained at a chemoturbine outlet pressure of 20 bar.

3.7 Conclusions

Two oxygen-based ethylene oxide processes were modelled. Both include steam cycles for power generation from the reaction heat recovered by reactor cooling. The generated power is used to supply part of the process' compression power.

In the second process, a chemoturbine is inserted at the reactor outlet. Two operating pressures were changed to accommodate the chemoturbine: The reactor pressure was increased to 40 bar and the ethylene oxide absorber pressure was decreased to 10 bar. With these process modifications, the net power requirement for the process can be reduced by 93% to 1.4 MW.

A sensitivity analysis showed that the power requirement can be reduced further and that 7.2MW of power can even be exported from the process.

Furthermore, there are specific pressure ratios (0.45 and larger) for which the chemoturbine alone can supply enough power to drive the recycle compressor. This proves that under certain operating conditions, expansion, separation and recompression schemes can deliver power for external use.

Chapter 4: Phthalic Anhydride Production

4.1 Introduction

Phthalic anhydride (PA) is produced from alkyl-substituted or multinuclear aromatic compounds by partial oxidation. Like other partial oxidation reactions, this reaction is highly exothermic and it presents opportunities for energy recovery.

Other characteristics that make this process interesting include a substantial pressure differential between the reaction and separation units for the insertion of a chemoturbine. Furthermore the aromatic compound is pumped to the reactor as a liquid (pumping a liquid requires only a fraction of the work required to compress a gas). No recycle or recompression is required because a high reactant conversion is achieved in a single reactor pass.

One negative aspect associated with the process is the stringent control of the reaction temperature. Isothermal reactor operation requires continuous heat removal leaving a smaller amount of heat to recover in the chemoturbine.

Two flowsheets are developed in Aspen: both include a Rankine-type steam cycle to produce power from the heat removed during the reaction. The second model also includes a chemoturbine for additional power production. The power produced in the two processes is compared over a variety of reaction conditions. An exergy analysis of the best process is also performed to identify areas where further improvements are possible.

4.2 The Reaction

Naphthalene can be catalytically oxidised to produce phthalic anhydride according to the reaction (Lorz *et al.*, 2001):

$$C_{10}H_8 + \tfrac{9}{2}O_2 \rightarrow C_8H_4O_3 + 2H_2O + 2CO_2 \qquad (10)$$

The reaction is extremely exothermic with a reaction heat of -1 793 kJ/mol (at 25°C). High yields can be achieved with reported values ranging from 90 kg PA/100 kg naphthalene (Ryder, Ryan & Klapproth, 1974: 5) to 102 kg PA/100 kg naphthalene (Lorz *et al.*, 2001) equivalent to 78 and 88 mol% conversion respectively. Three competing reactions of significance are:

the formation of naphthoquinone (an intermediate in PA production)

$$C_{10}H_8 + \tfrac{3}{2}O_2 \rightarrow C_{10}H_6O_2 + H_2O \qquad (11)$$

the formation of maleic anhydride (MA)

$$C_{10}H_8 + 6O_2 \rightarrow 2C_4H_2O_3 + 2H_2O + 2CO_2 \qquad (12)$$

as well as naphthalene combustion (Lorz *et al.*, 2001)

$$C_{10}H_8 + 12O_2 \rightarrow 4H_2O + 10CO_2 \qquad (13)$$

Two reactor configurations are used for phthalic anhydride production: multitubular fixed bed and fluidised bed reactors. Conversions are slightly higher when tubular reactors are used, but the temperature control in fluidised beds is better and flammability problems are less likely to occur (Lorz *et al.*, 2001). The latter type of reactor will be considered further because of its higher operating pressures (3.4 to 35 bar). Reaction temperatures are usually maintained between 320 and 400°C with higher temperatures favouring complete combustion (Ryder *et al.*, 1974: 2).

4.3 Production Process

A process flowsheet for a plant producing phthalic anhydride via the catalytic oxidation of naphthalene is shown in Figure 6.

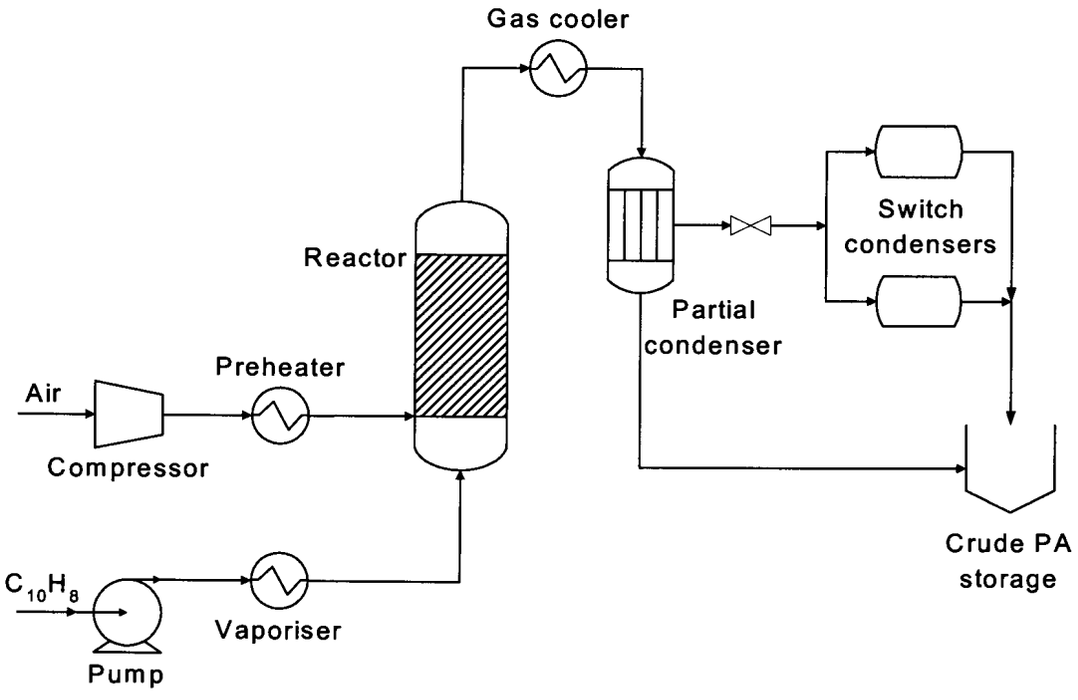

Figure 6: Flowsheet for phthalic anhydride production using a fluidised bed reactor (from Ryder *et al.*, 1974: 2)

Air and naphthalene are brought to the reactor pressure by a compressor and pump respectively. The air is then preheated and naphthalene vaporised before entering the reactor (Ryder, 1974: 5). As an alternative, liquid naphthalene can also be injected into the reactor where it will vaporise instantly (Lorz *et al.*, 2001).

The fluidised reactor is maintained at a temperature of 320-400°C and a pressure of 3.4 to 35 bar. Heat liberated by the reaction is removed by the direct generation of steam in the reactor cooling coils. The steam pressure is typically in the range of 7 to 28 bar (Kunii & Levenspiel, 1991: 28).

The reaction product is cooled to a temperature just above the dew point of phthalic anhydride. This is followed by a partial condenser that removes roughly half of the phthalic anhydride as liquid. The liquid product is sent to a storage tank where it awaits final purification.

The gaseous product from the partial condenser proceeds to one of two switch condensers. These units operate batch wise and have cooling and heating cycles. During the cooling cycle, the gaseous mixture is cooled down and phthalic anhydride deposits as a solid product. The remaining gasses are removed from the switch condenser and are sent to an air treatment facility (not shown). During the heating cycle, the phthalic anhydride melts and flows to the storage tank.

Final purification of the liquid phthalic anhydride occurs in two distillation columns operating at sub atmospheric pressures (Deutner & Neumann, 1975: 2). Maleic anhydride is usually removed as the distillate of the first column and phthalic anhydride as the distillate of the second column. Naphthoquinone and other high boiling compounds are recovered at the bottom of the second column.

Current advances in PA production technology are focused on minimising energy consumption. This includes efforts to use the large amounts of steam (raised during the reactor cooling) by driving the air compressor with a steam turbine (Lorz *et al.*, 2001).

4.4 Process Modelling

4.4.1 Assumptions and Constraints

Based on the range of operating conditions mentioned in section 4.2 and 4.3, as well as the type of components in the system (predominantly nonpolar), the Soave Redlich Kwong equation of state was specified as the property method. The STEAMNBS property method was used for the steam cycle flowsheet subsection.

Component data for naphthoquinone is not present in the Aspen Plus databanks and hence it was omitted from the simulation. As an intermediate in the production of phthalic anhydride (reaction 11), it is not commonly observed in the final product. It is expected that the results would not be influenced significantly with this omission.

Pressure drop in the reactor, mixer, heat exchanger and separator units were considered negligible. All the process units were assumed to be well insulated to eliminate heat loss to the environment.

4.4.2 Process without a Chemoturbine (Case A)

A steady state model of a phthalic anhydride plant was developed with Aspen. The process flowsheet is shown in Figure 7. It is similar to Figure 6, but includes a Rankine-type steam cycle and distillation column.

The turbine in the steam cycle (see Figure 8) supplies power to the air compressor while the distillation column separates maleic and phthalic anhydride.

The various unit processes used in the simulation model are discussed in the remainder of this section.

Feed streams

The temperatures, pressures and compositions of the feed streams used in the simulations are shown in Figure 9.

Naphthalene liquid is pumped to the reactor pressure and vaporised before entering the reactor.

Air is compressed in a two-stage compressor with intercooling to 25°C. Aspen's default isentropic efficiency of 72% was used.

Before entering the reactor, the air is preheated to 150°C as prescribed (Ryder *et al.*, 1974: 5). An air to naphthalene ratio of 11.3:1 (by weight) was used.

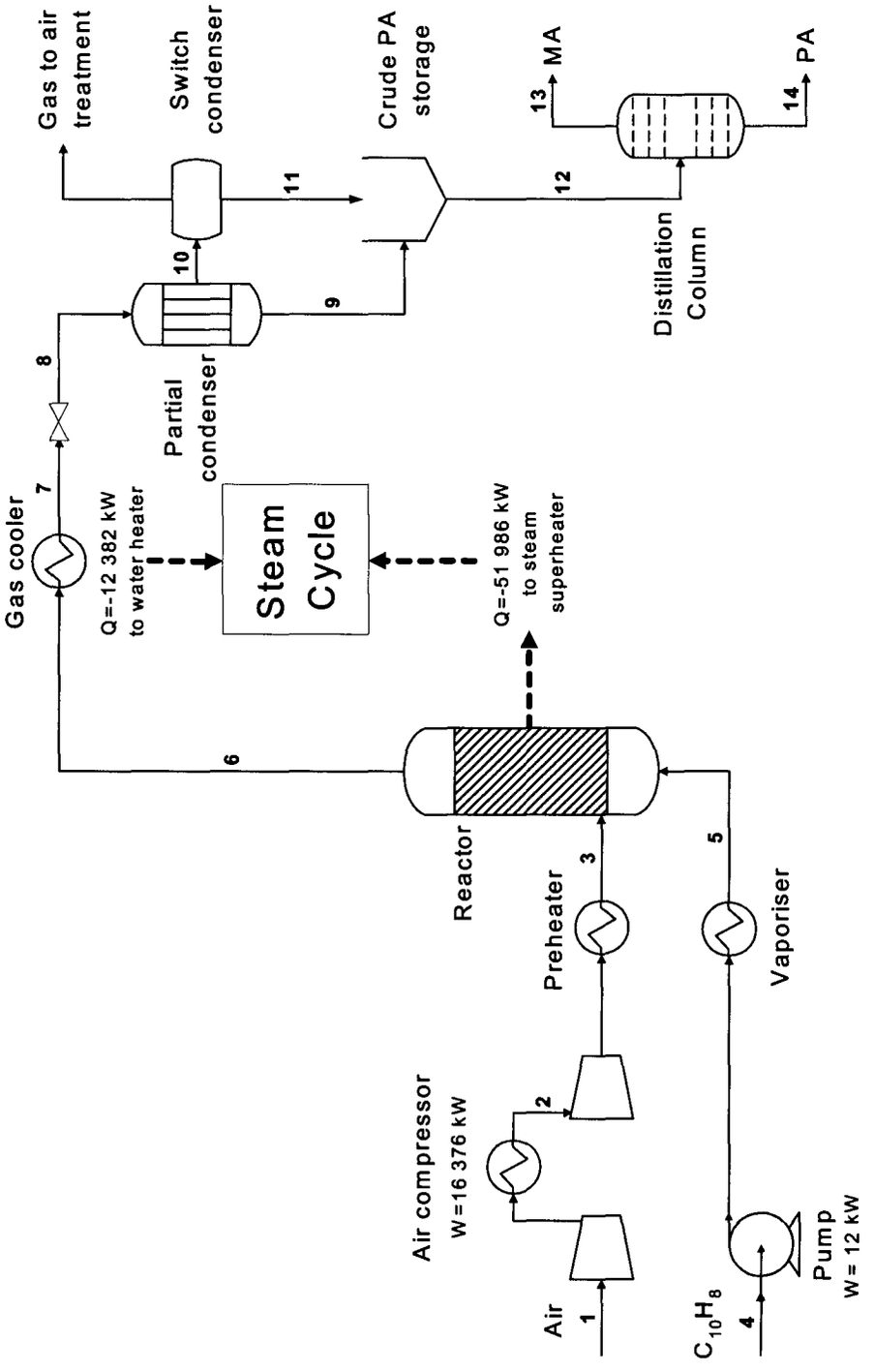

Stream number	1	2	3	4	5	6	7	8	9	10	11	12	13	14
Temperature (°C)	25	25	187	25	387	400	176	160	160	160	131	144	142	233
Pressure (Bar)	1	5	16	1	16	16	16	1.8	1.8	1.8	1.4	1.4	0.1	0.25
Mole Flow (kmol/h)	5 000	5 000	5 000	100	100	5 082	5 082	5 082	41	5 041	53	94	19	75
Mass Flow (ton/h)	144.3	144.3	144.3	12.8	12.8	157.1	157.1	157.1	6.0	151.1	7.1	13.1	2.0	11.1

Figure 7: Flowsheet of the phthalic anhydride process as simulated in Aspen Plus

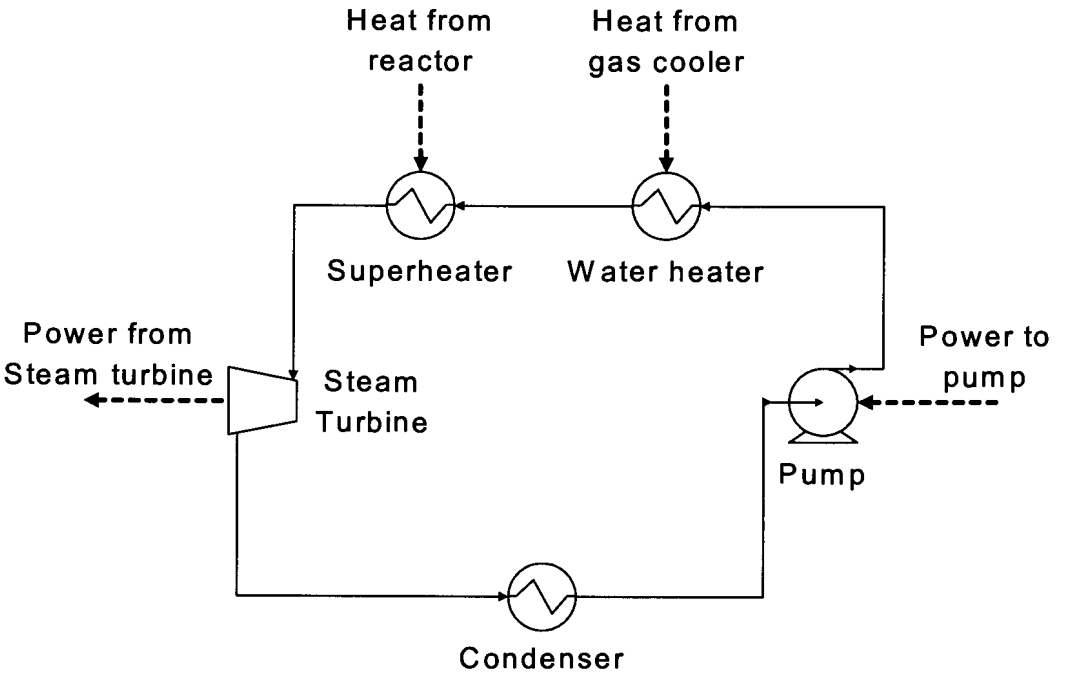

Figure 8: Steam cycle as simulated in Aspen Plus

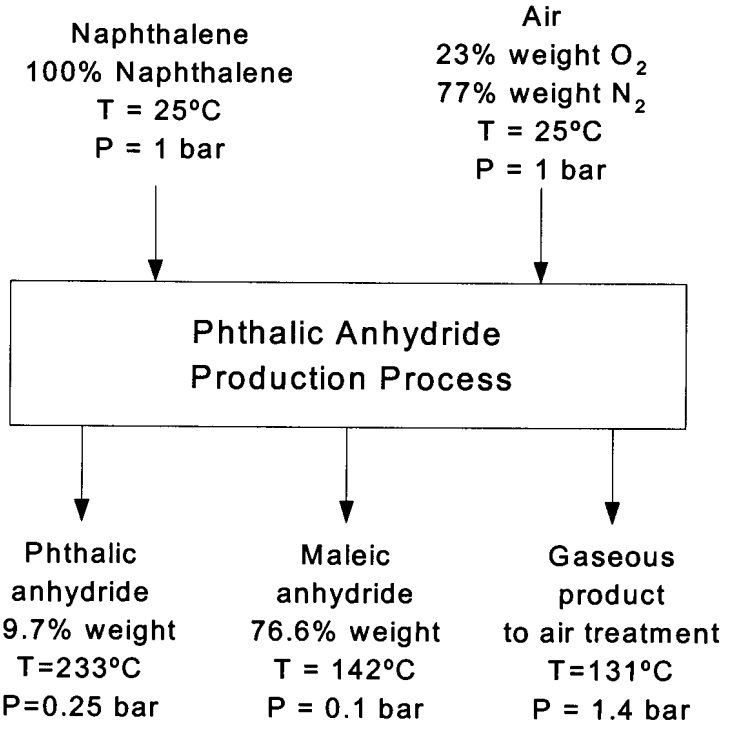

Figure 9: Feed and product streams for the phthalic anhydride simulations

Reactor

The fluidised bed reactor was modelled as an isothermal reactor. No reliable set of reaction kinetics could be found because researchers disagree on the reaction order of naphthalene (Wainwright & Foster, 1979: 236). Hence, a stoichiometric reactor model was used instead. The conversion specifications for the simulation model are shown in Table 5.

Table 5: Reaction conversion specifications for the reactor model

Reaction		Conversion
$C_{10}H_8 + 4.5O_2$	$\rightarrow C_8H_4O_3 + 2CO_2 + 2H_2O$	78%
$C_{10}H_8 + 6O_2$	$\rightarrow 2C_4H_2O_3 + 2CO_2 + 2H_2O$	8%
$C_{10}H_8 + 12O_2$	$\rightarrow 10CO_2 + 4H_2O$	11%
$C_{10}H_8 + 7O_2$	$\rightarrow 10CO + 4H_2O$	3%

The conversion to phthalic anhydride of 78% translates to 90 kg phthalic anhydride/100 kg naphthalene as mentioned by Ryder *et al.* (1974: 5).

Simulations were carried out with the reactor conditions varying between three temperatures and pressures namely 320, 365 and 400°C and 8, 12 and 16 bar. The conversion specifications of Table 5 (i.e. constant conversions and selectivities) were used at all the conditions investigated. Although this is only an assumption, the fact that it is used in all the processes means that relative comparisons can still be made. A reliable set of kinetics would be required for a detailed design of any one of the conceptual flowsheets.

Gas Cooler

This heat exchanger is used to cool the reactor product to a temperature slightly above the dew point of the phthalic anhydride in the mixture. At a pressure of 1.8 bar, this corresponds to a temperature of about 160°C. The recovered heat is used to heat water for the steam cycle (see Figure 8).

Expansion valve

The product cooler operates at the reactor pressure, but the separation steps are carried out at lower pressures. An isenthalpic expansion valve is used to lower the pressure to 1.8 bar, the pressure at which the partial condenser operates.

Partial condenser

Almost half of the phthalic anhydride can be recovered in liquid form from the partial condenser (Ryder *et al.*, 1974: 5) but this depends on the unit's operating pressure. In the flash drum used in the model, this kind of separation was achieved at a pressure of 1.8 bar and a temperature of 160°C.

At the chosen operating conditions, the total mole fraction of N_2, O_2, CO, CO_2 and water in the liquid product was 0.8%. This value seems insignificant, but it was enough to create numerical instability for the downstream distillation column. To resolve this problem the flash drum was replaced by a black box separator. Flash specifications were kept constant, but a separation efficiency of 100% was specified for N_2, O_2, CO, CO_2. Mass and energy balances were not affected in a noteworthy manner.

Switch condenser

Modern condensers can separate more than 99.5 % of the phthalic anhydride from the reaction gas (Lorz *et al.*, 2001). With this high degree of separation, it was decided to use another black box separation block to model this unit. Maleic and phthalic anhydride were specified to be the only components allowed to leave in the liquid phase at 131°C and 1.4 bar. The remaining compounds leave in the gaseous phase and proceed to an air treatment facility (not considered).

Distillation column

Separation of maleic and phthalic anhydrides takes place in a distillation column. Phthalic anhydride is recovered as the bottom product with a weight purity of 99.7%. This is the typical purity available commercially (Herdillia Chemicals, 2001).

Due to the absence of naphthoquinone and other high boiling compounds, the second column mentioned in section 4.3, became redundant.

Power cycle

The steam generated through the cooling of the reactor is used to produce power in a Rankine-type steam cycle. An overview of Rankine cycles is given in Appendix C.

The steam cycle scheme shown in Figure 8 was employed. The high temperature heat utilised include the heat removed from the reactor as well as the heat released upon cooling the reaction product. The reactor product was used to heat cold water whilst the reactor heat was used to vaporise and superheat the hot water.

Cooling water at 15°C and ambient pressure was used to remove heat from the condenser. Other specifications for the steam cycle calculations are shown in Table 6.

Table 6: Steam cycle specifications

Parameter	Value	Units
Temperature driving force for vaporiser/superheater	20[a]-35	°C
Temperature driving force for condenser	20	°C
Steam turbine inlet pressure	28	bar
Steam turbine outlet pressure	0.15-0.2[a]	bar
Steam turbine isentropic efficiency	75	%
Maximum liquid fraction at turbine outlet[b]	0.1	-
Degrees of subcooling in condenser	5	°C
Pump isentropic efficiency	100	%

[a] Specification when reaction temperature is 320°C

[b] Limit commonly applied in practice (Winnick, 1997: 177)

Three Aspen design specification routines were used. The first ensured that the temperature driving force specification for the superheater was met whilst the second controlled the liquid fraction at the turbine outlet. The flow rate of the steam in the cycle was optimised for maximum power generation. The third routine calculated the cooling water flow rate required to remove the low temperature heat from the condenser.

4.4.3 Process with a Chemoturbine (Case B)

After the simulations for Case A, the model was changed by placing a chemoturbine directly after the reactor. This change is shown on the flowsheet in Figure 10.

The changes in the flowsheet due to the inclusion of the chemoturbine are discussed below.

Chemoturbine

The chemoturbine operates with an efficiency of 72% compared to isentropic operation. This efficiency value is the default used by Aspen. The outlet pressure of 1.8 bar was specified to coincide with the partial condenser operating pressure. By choosing this particular outlet pressure, no downstream unit operations have to change with the inclusion of the chemoturbine.

Unlike the steam turbine where a 10% liquid fraction was allowed, no liquid is allowed to form in the chemoturbine. In three simulations where liquid presence was predicted, the turbine's outlet pressure was increased until this was no longer the case. The particular cases where this occurred, as well as the adjusted outlet chemoturbine pressure are given in Table 7. The remainder of the pressure drop to 1.8 bar occurred via an expansion valve similar to the one used in Case A.

Table 7: Adjusted outlet pressure for cases where condensation occurred

Reactor conditions		Chemoturbine outlet pressure
Temperature	Pressure	
320°C	12 bar	2.5 bar
320°C	16 bar	3.9 bar
365°C	16 bar	1.9 bar

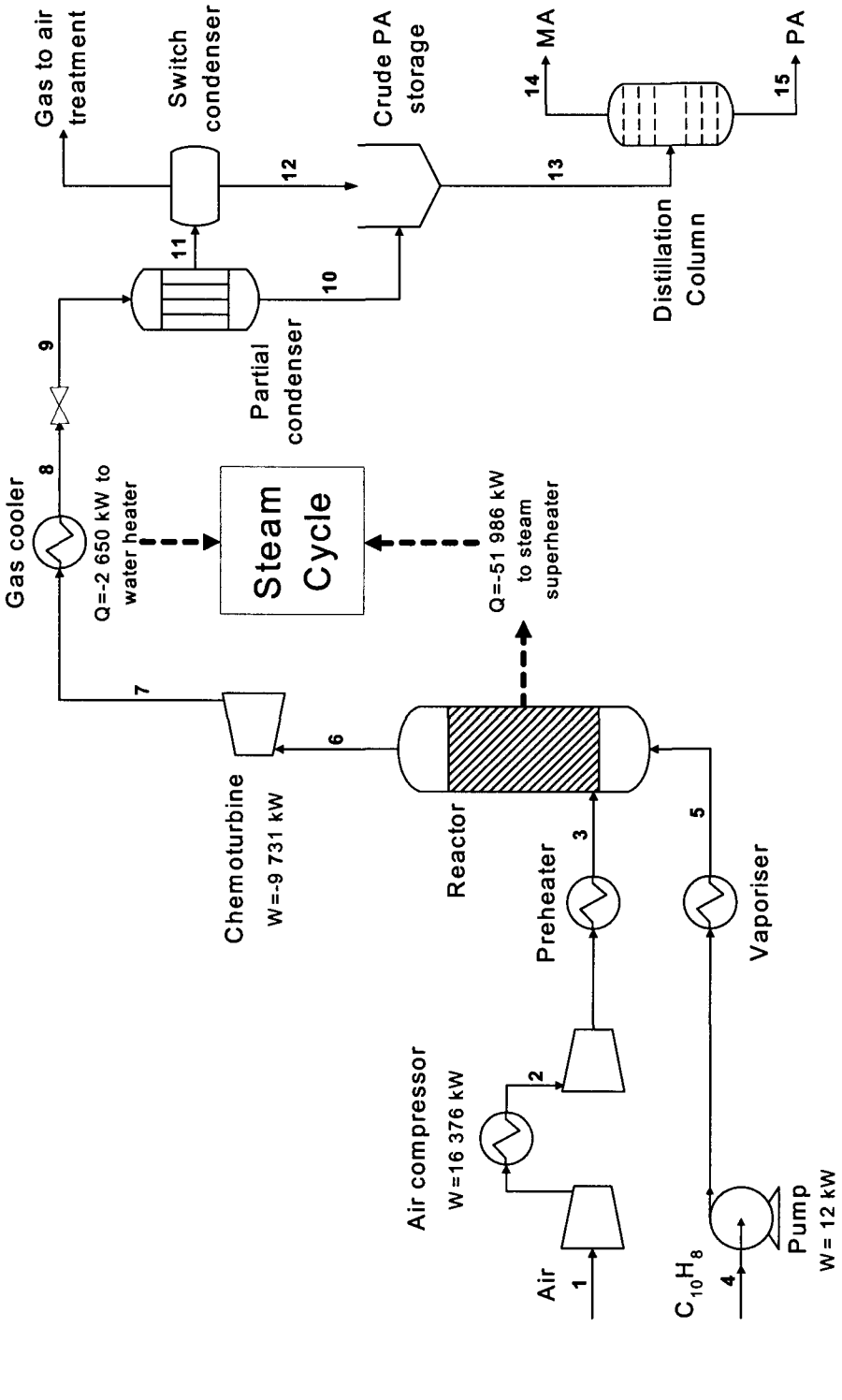

Stream number	1	2	3	4	5	6	7	8	9	10	11	12	13	14	15
Temperature (°C)	25	25	186.6	25	386.5	400	198.9	160	160	160	160	131	143.9	141.9	233
Pressure (Bar)	1	5	16	1	16	16	1.8	1.8	1.8	1.8	1.8	1.4	1.4	0.1	0.25
Mole Flow (kmol/h)	5 000	5 000	5 000	100	100	5 082	5 082	5 082	5 082	41	5 041	53	94	19	75
Mass Flow (ton/h)	144.3	144.3	144.3	12.8	12.8	157.1	157.1	157.1	157.1	6.0	151.1	7.1	13.1	2.0	11.1

Figure 10: Flowsheet of the phthalic anhydride process with chemoturbine as simulated in Aspen Plus

4.5 Comparison of Case A and Case B

4.5.1 Net Power Production

The power consumed by the feed compressor and pump are summarised alongside the power generated from the steam cycle and chemoturbine in Table 8.

Table 8: Comparison of net power generated

	Case A & B	Case A		Case B			
Reaction Temp. (°C)	Feed pump and compressor power (kW)	Steam cycle power (kW)	Net power (kW)	Steam cycle power (kW)	Chemo-turbine power (kW)	Chemoturbine contribution to total power (%)	Net power (kW)
Reaction pressure = 8 bar							
320	12 176	-14 046	-1 870	-12 646	-6 297	33	-6 767
365	12 176	-14 692	-2 516	-13 098	-6 757	34	-7 679
400	12 176	-14 874	-2 698	-13 164	-7 141	35	-8 129
Reaction pressure = 12 bar							
320	14 679	-14 106	573	-12 613	-6 592	34	-4 526
365	14 679	-14 716	-37	-12 790	-8 253	39	-6 364
400	14 679	-14 928	-250	-12 856	-8 686	40	-6 862
Reaction pressure = 16 bar							
320	16 387	-14 115	2 272	-12 776	-6 038	32	-2 427
365	16 387	-14 751	1 636	-12 622	-9 078	42	-5 313
400	16 387	-14 964	1 423	-12 645	-9 731	43	-5 990

There are sets of operating conditions for which the steam cycle in Case A cannot supply all of the power required for compression and power has to be imported from an external source. In Case B, there is a net power production for all the conditions investigated (i.e. power can be exported to other processes).

The first trend to be noticed is that the net power production increases with an increase in reaction temperature. This is expected as both the steam cycle and chemoturbine deliver more power at higher reaction temperatures.

The higher net power production at lower pressures is less obvious. With the power generated by the steam cycle more or less independent of pressure, this observation is most likely due to the increments in compression power being larger than that of chemoturbine power. On comparison of the incremental increases of the feed compression and chemoturbine power, one can see that this is indeed the case. Increases in the former are roughly 40% larger for each pressure increase of four bar.

4.5.2 First Law Analysis

The term "First law analysis", as it is used here, refers to the evaluation of the changes in energy that occur in the process and more specifically to the conversion of high temperature heat to power. This is done by means of the thermal conversion (TC) efficiency, defined below.

Given the high number of efficiency definitions reported in literature one should always apply them with caution. Hence, the thermal conversion efficiency used to compare Case A and B was defined with one objective in mind: to give a quantitative value for comparing the conversion of high temperature heat from the exothermic reaction to power.

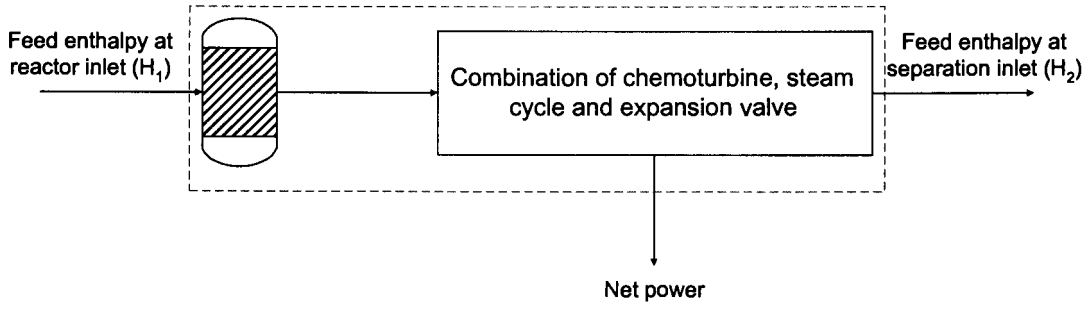

Figure 11: System boundaries for the definition of thermal conversion efficiency

System boundaries for the thermal conversion efficiency are shown in Figure 11 by dashed lines. The change in enthalpy between the reactor and separator inlet conditions (H_1 and H_2 respectively) acts as the high temperature heat source whilst the net power is the sum of the power from the chemoturbine and steam turbine less that required to drive the pump in the steam cycle. In mathematical terms, the thermal conversion efficiency is written as:

$$\eta_{TC} = \frac{\dot{W}_{chemoturbine} + \dot{W}_{steam\ turbine} - \dot{W}_{steam\ cycle\ pump}}{H_1 - H_2} \qquad (14)$$

It may be argued that this efficiency definition does not include the feed compression requirements as in a typical power cycle (Winnick, 1997: 174), but it has already been shown in section 4.5.1 that some cases have a negative net power production. (i.e. net power input). Such systems are better evaluated by a "Coefficient of Performance" similar to that used in heat pump analysis (Winnick, 1997: 74). The inclusion of the compression work would therefore necessitate the use of a second performance parameter that would complicate the analysis.

Thermal conversion efficiencies were calculated for Case A and B over the range of temperatures and pressures investigated, the results of which are depicted in Figure 12 and Figure 13 respectively.

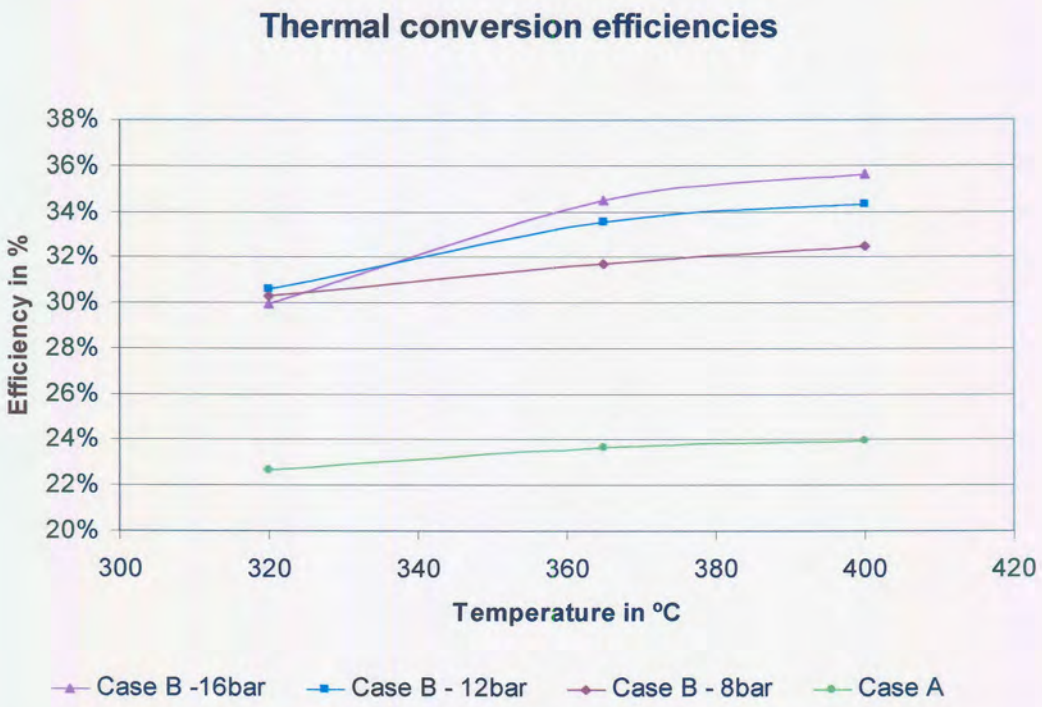

Figure 12: Thermal conversion efficiencies as functions of reaction temperature

The efficiencies are plotted against reaction temperature in Figure 12. A single thermal conversion efficiency is reported for the Case A, as its steam cycle is

independent of reaction pressure. One can see that Case B gives efficiency increases of at least 7% over Case A.

Both efficiencies increase with increasing reaction temperature. This is expected with isothermal reactor operation because an increase in the reaction temperature means that less heat is removed from the reactor and the reaction product enthalpy is higher. With the chemoturbine exiting conditions (and hence enthalpy) remaining constant through most of the simulations, the increase in the turbine's inlet enthalpy translates directly into higher power production.

It is further interesting to note that higher operating pressures (i.e. higher pressure ratios) result in higher efficiencies for Case B. Recall from section 4.5.1 that lower pressures resulted in higher net power production. This means that there is a trade-off between efficiency and net power production. This behaviour is typical for Brayton cycles.

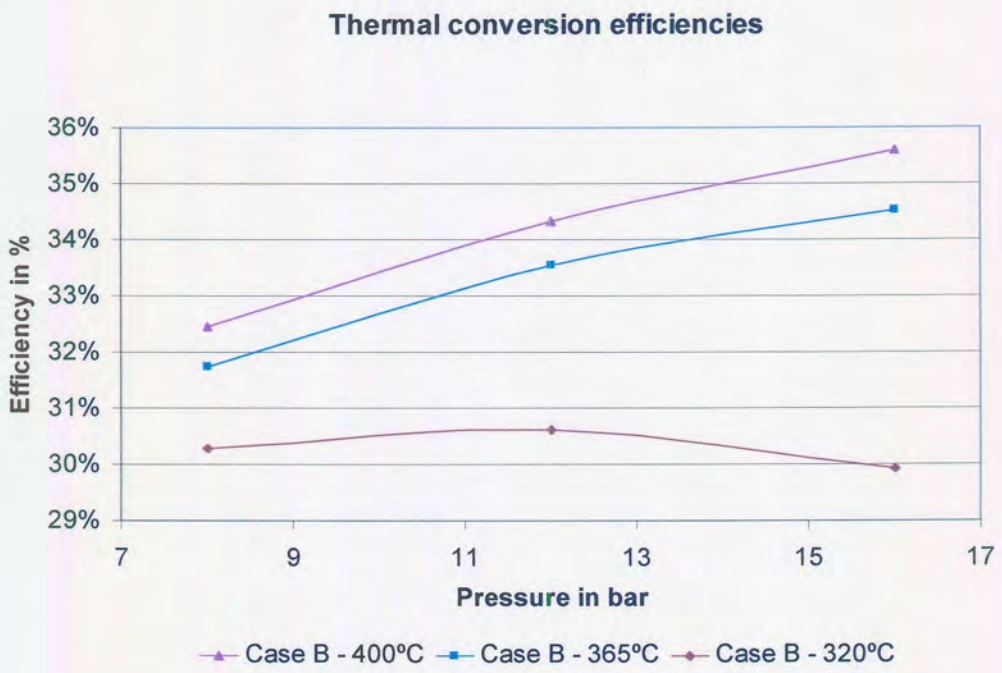

Figure 13: Thermal conversion efficiencies as functions of reaction pressure

It has already been mentioned that pressure increases have a beneficial effect on the power production of the chemoturbine. This is confirmed in Figure 13. The 320°C

curve appears to have a maximum that is not observed for the other two curves, but, as explained earlier, this is due to a change in outlet conditions to avoid condensation within the chemoturbine.

4.5.3 Exergy Analysis

An exergy analysis was performed for Case A and B at the reactor conditions of 400°C and 16 bar. The highest net power production is not achieved at these conditions, but the contribution of the chemoturbine to the total power is the highest (43%) and it also has the highest thermal conversion efficiency (36%). The boundary conditions shown in Figure 11 were used again as this is the only section where differences exist between the two processes.

Prior to performing the exergy calculations, the standard chemical exergy of maleic anhydride was calculated as it is not included in the Exercom databases. The calculations are shown in Appendix D.

The degree of perfection (DOP) as described in section 2.3 was used to quantify the exergy efficiency of the processes. The mathematical formulation of (4) for the subsection under consideration is given by:

$$\eta_{DOP} = \frac{\dot{E}_{\text{partial condenser feed}} + \dot{W}_{\text{chemoturbine}} + \dot{W}_{\text{steam turbine}}}{\dot{E}_{\text{reactor air feed}} + \dot{E}_{\text{reactor naphthalene feed}} + \dot{E}_{\text{condenser cooling liquid}} + \dot{W}_{\text{steam cycle pump}}} \qquad (15)$$

The cooling liquid from the condenser is not included in the numerator of equation 15. With a temperature of only 40°C, it is not considered to be of value for use elsewhere.

Under these conditions, the degree of perfection was 58.7% and 63.2% for Case A and B respectively. For a more detailed view of where the exergy is lost, refer to Figure 14. It shows the irreversibility rate for each of the unit operations within the boundary conditions.

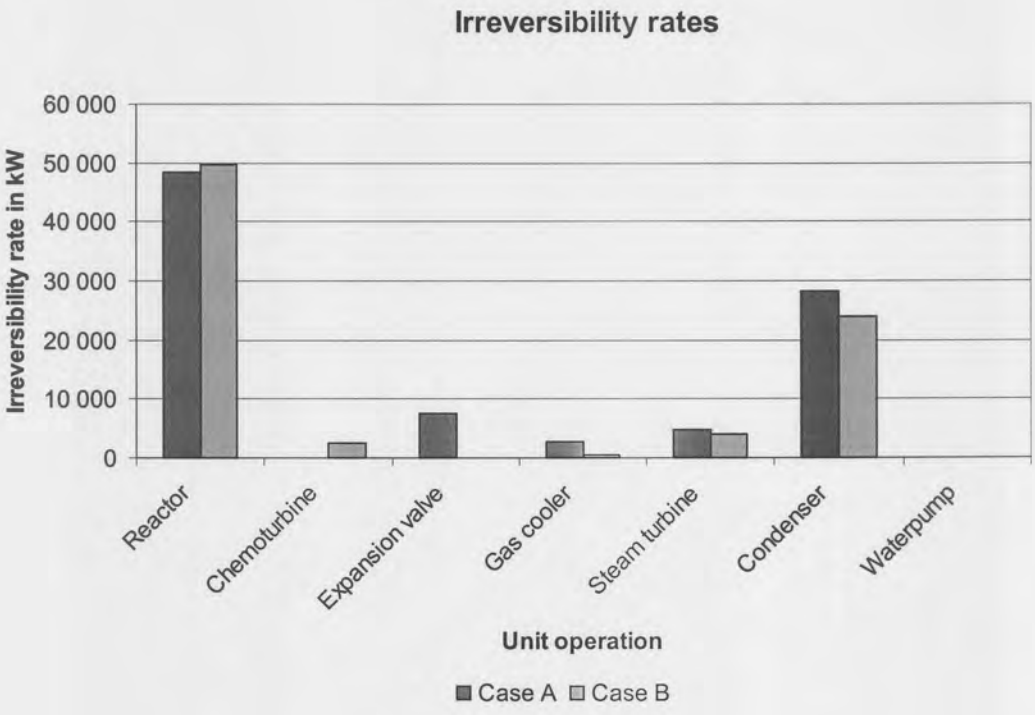

Figure 14: Comparison of irreversibility rates per unit operation

Two unit operations have particularly large irreversibility rates: the reactor and the condenser in the steam cycle. If the processes were to be improved further, it would be best to focus on these two units.

The irreversibility rate in the reactor is slightly higher for Case B. This is due to the lower temperature of the boiler feed water (84°C compared to 183°C for Case A). The large difference between these two temperatures exists because a temperature decrease takes place in the chemoturbine resulting in a lower temperature to heat boiler feed water. In Case A, boiler feed water can be heated with heat at the reactor temperature.

The fact that the cooling water is not considered a valuable product is the main reason why the irreversibility rate of the condenser is so high. However, with a temperature of only 40°C, opportunities for its use elsewhere are limited.

The benefit of the chemoturbine can be seen when looking at the third highest irreversibility rate in Case A. It occurs in the expansion valve. Although an energy

balance over this unit will show it to be 100% efficient, one can now see that losses do occur in this unit as a result of the pressure decrease. In Case B, this pressure reduction takes place in the chemoturbine. The exergy loss associated with the chemoturbine is smaller because a valuable product, power, is also obtained.

4.6 Conclusions

Two phthalic anhydride processes were simulated. Both include a steam cycle to recover reaction heat in the form of power. This power is used to drive the feed compressor and pump. In the second process, a chemoturbine was included for additional power production.

Results show that, without the presence of the chemoturbine, there are certain operating conditions where the steam cycle alone cannot supply the full amount of feed compression power. Hence, power has to be imported from an external source. Upon the inclusion of the chemoturbine this situation changes and power can even be exported for use elsewhere. Depending on the reactor operating conditions, as much as 8.1 MW can be exported from the process.

Comparing processes where power is imported under certain conditions and exported under others are difficult, because efficiency definitions usually apply to only one of these situations. This problem is avoided in the thermal conversion efficiency employed here. It does not include feed compression power, but its use is limited to the characterisation of the energy conversion efficiency from a high temperature heat source to power. For the conditions investigated, a maximum thermal conversion efficiency of roughly 36% is possible when the process includes a chemoturbine. Reactor operating conditions corresponding to this efficiency value are 400°C and 16 bar.

The exergy analysis showed that the degree of perfection of the process could be improved by 4.5% (from 58.7% to 63.2%) when the pressure reduction takes place in a chemoturbine instead of the expansion valve. It is also a helpful tool to determine which unit operations should be looked at more carefully to further improve the

process. In the present situation, the reactor and condenser have the largest irreversibility rates and should be considered first.

Chapter 5: Hydrodealkylation of Alkylaromatic Compounds

5.1 Introduction

As seen from the previous chapters, flowsheet changes have to be made when a chemoturbine is added to a process. In this chapter, a new conceptual flowsheet, that includes a chemoturbine for reaction heat recovery, is developed for a hydrodealkylation (HDA) process.

The HDA process was chosen for this conceptual design because it exhibits the following characteristics:

- high exothermic reaction heat and adiabatic temperature rise over the reactor
- availability of reaction kinetics and process data
- large difference between the reaction and separation pressures

Besides designing the new flowsheet, additional simulations were conducted to improve its performance. Three alternatives were considered to reduce the reactor residence time and a sensitivity analysis was performed to determine whether more power could be obtained from the process.

This work was carried out in cooperation with the following Dutch institutions: Dow Chemicals Benelux (Dow), Kema Power Generation and Sustainables, the Netherlands Organisation for Applied Scientific Research and the Technical University of Eindhoven.

5.2 The Reactions

Hydrodealkylation refers to the removal of alkyl groups from an organic compound, and in this particular case, from aromatic compounds such as toluene, xylene and ethylbenzene. The reactions (16 through 18) take place in the vapour phase in the presence of an excess of hydrogen (Luijten, 2000). Benzene is the main product from

these reactions with lower alkane compounds (predominantly methane and ethane) as by-products.

Toluene HDA: $C_7H_8 + H_2 \rightarrow C_6H_6 + CH_4$ (16)

Ethylbenzene HDA: $C_8H_{10} + H_2 \rightarrow C_6H_6 + C_2H_6$ (17)

Xylene HDA: $C_8H_{10} + 2H_2 \rightarrow C_6H_6 + 2CH_4$ (18)

Heavy aromatic compounds (aromatic compounds with molecular weights in excess of 106) are also formed through side reactions that include (Luijten, 2000):

Biphenyl formation: $2C_6H_6 \leftrightarrow C_{12}H_{10} + H_2$ (19)

Naphthalene formation: $2C_6H_6 + H_2 \rightarrow C_{10}H_8 + 2CH_4$ (20)

Methylbiphenyl formation: $C_6H_6 + C_7H_8 \leftrightarrow C_{13}H_{12} + H_2$ (21)

Dimethylbiphenyl formation: $2C_7H_8 \leftrightarrow C_{14}H_{14} + H_2$ (22)

Besides reducing the benzene output from the system, these heavy aromatic compounds can build up and deteriorate heat transfer. Careful control of the reactor conditions is required to minimise the formation of these compounds.

The reactions are carried out adiabatically in a tubular reactor without a catalyst. Reaction pressures are in the range of 55 to 60 bar and inlet temperatures are usually in the order of 600°C. Adiabatic temperature rises of 130°C are common as the majority of the reactions that take place are exothermic. The conversion of toluene, ethylbenzene and xylene to benzene (overall aromatic conversion) is 95%. In practice, the production of heavy aromatics is minimised by using a molar feed ratio of hydrogen to aromatics of at least five (Luijten, 2000).

5.3 Flowsheet Design and Modelling

5.3.1 Typical Process for the Hydrodealkylation of Aromatic Compounds

Figure 15 shows a flowsheet with compression, reactor, separation and a recycle loop as typically used for the HDA process. The type of separation is not specified yet, but a flash drum and cryogenic separation are usually employed (Luijten, 2000). No heat exchangers are shown in the flowsheet. They will be added as the flowsheet is developed.

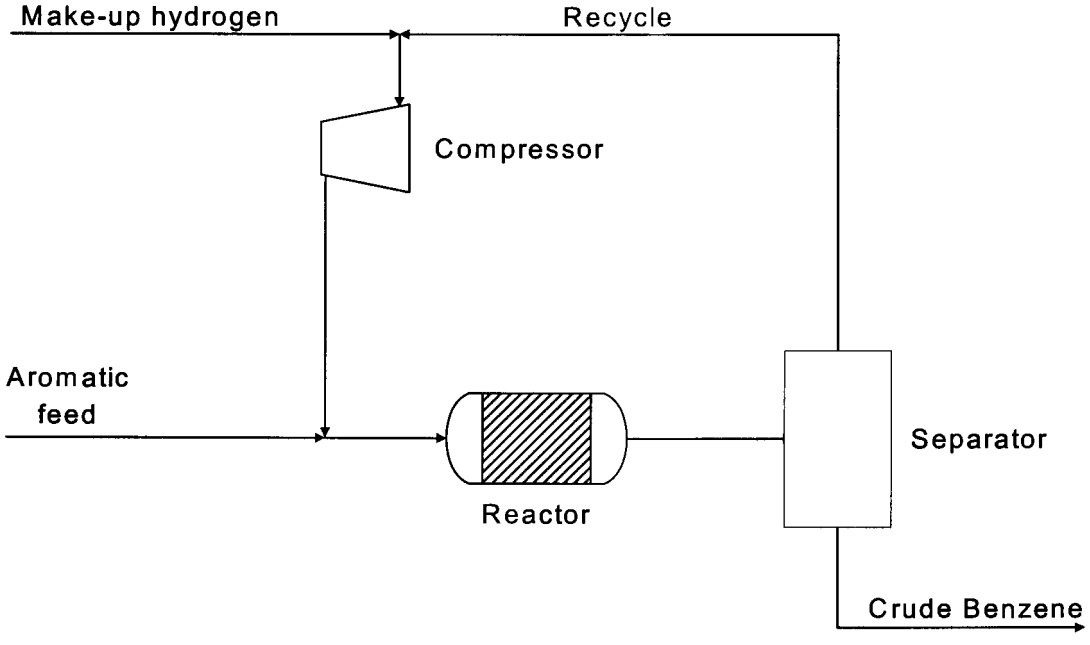

Figure 15: Process flowsheet with separation and compression steps

The new flowsheet was developed with Figure 15 as starting point. The following information was obtained from a conventional industrial process to aid in the flowsheet development:

- data regarding typical make-up and recycle stream compositions, temperatures and pressures.
- reaction conditions (inlet temperature, pressure, residence time etc.)
- reaction kinetics

5.3.2 Assumptions and Constraints

Given that the system operates at very high temperatures (reactor outlet typically 730°C) and pressures (60 bar) and contains mostly nonpolar compounds, the Soave Redlich Kwong property method was preferred for thermodynamic property calculations.

All the process units were assumed to be well insulated to prevent heat loss to the environment. Pressure drop in the reactor, mixer, heat exchanger and separator units were considered negligible

One initial constraint was made: the pressure limits for the recycle loop was fixed at 30 and 60 bar respectively (Ploumen, 2000). The lower limit coincides with the pressure at which make-up hydrogen is fed to the process whilst the upper limit is the reaction pressure. The latter is usually between 55 and 60 bar (section 5.2). Reactor operation at 60 bar is expected to be more beneficial for power production due to the larger pressure drop (30 bar) over the chemoturbine (see equation B2 in Appendix B).

Through the insertion of a membrane separator, a methane rich stream of high purity (87 mol%) becomes available. Although this gas can be used to drive a gas turbine for additional power generation, its high purity makes it suitable as chemical feedstock for downstream processes (Luijten, 2000). Hence, a second constraint was added: high purity methane should be delivered to downstream processes at 19°C and 16 bar.

5.3.3 Flowsheet Development

The most appropriate position for the chemoturbine is directly after the reactor, at the highest temperature in the process. This is shown in Figure 16. The flowsheet was developed for this situation.

The remainder of this section is dedicated to the discussion of the flowsheet design. The discussion includes the operating conditions and other parameters specified for the unit operations as well as the reasoning behind each specification.

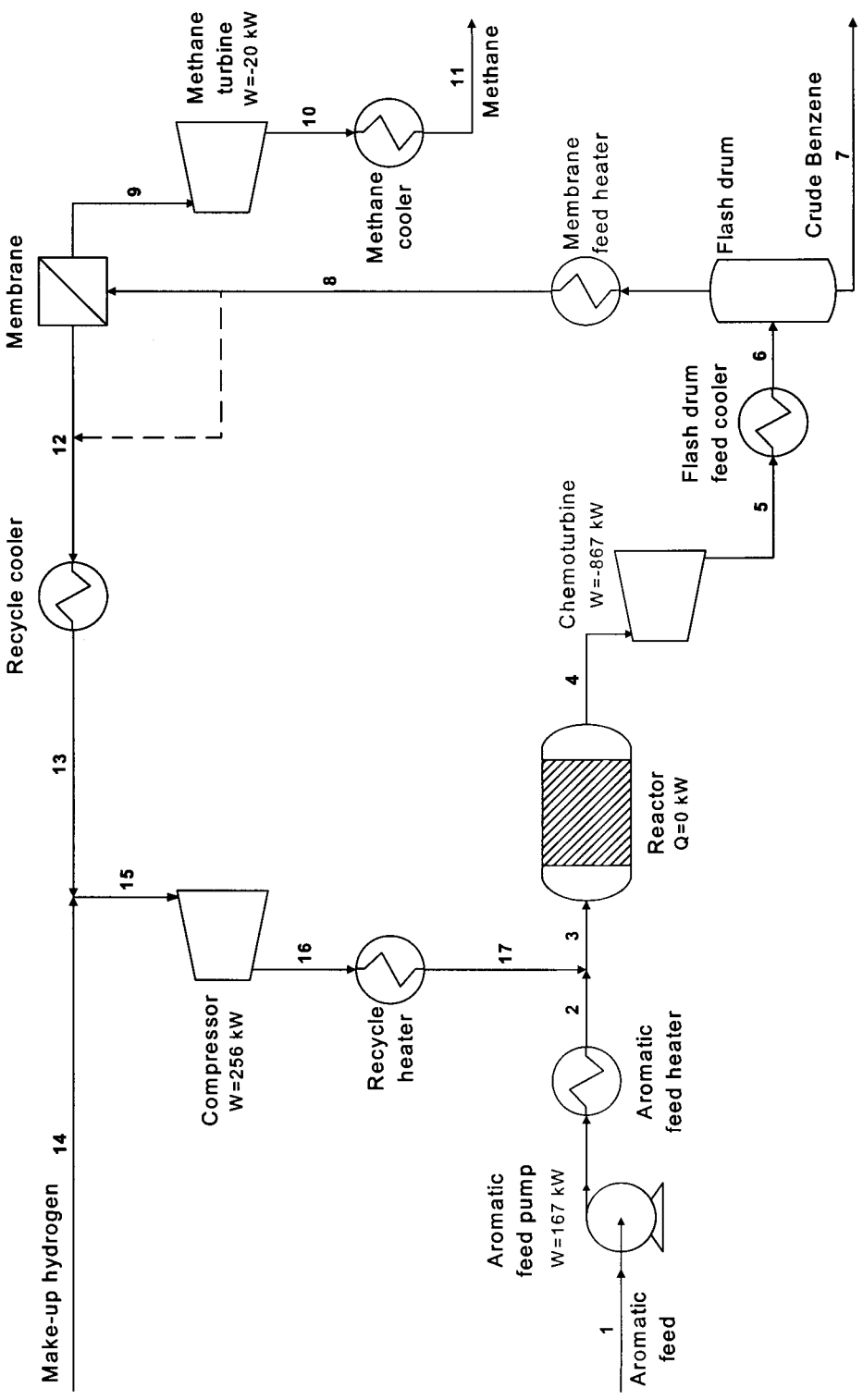

Stream number	1	2	3	4	5	6	7	8	9	10	11	12	13	14	15	16	17
Temperature (°C)	25	600	593	720	700	25	25	200	200	152	19	200	10	10	10	88	600
Pressure (Bar)	1	60	60	60	30	30	30	30	30	16	16	30	30	30	30	60	60
Mole Flow (kmol/h)	569	569	946	957	957	957	341	616	615	615	615	1	1	376	377	377	377
Mass Flow (kg/h)	56 000	56 000	58 017	58 017	58 017	58 017	46 896	11 121	11 104	11 104	11 104	17	17	2 000	2 017	2 017	2 017

Figure 16: Flowsheet for hydrodealkylation process as simulated in Aspen Plus

Make-up stream preparation

The temperatures, pressures and compositions of the make-up streams used in the simulations are shown in Figure 17.

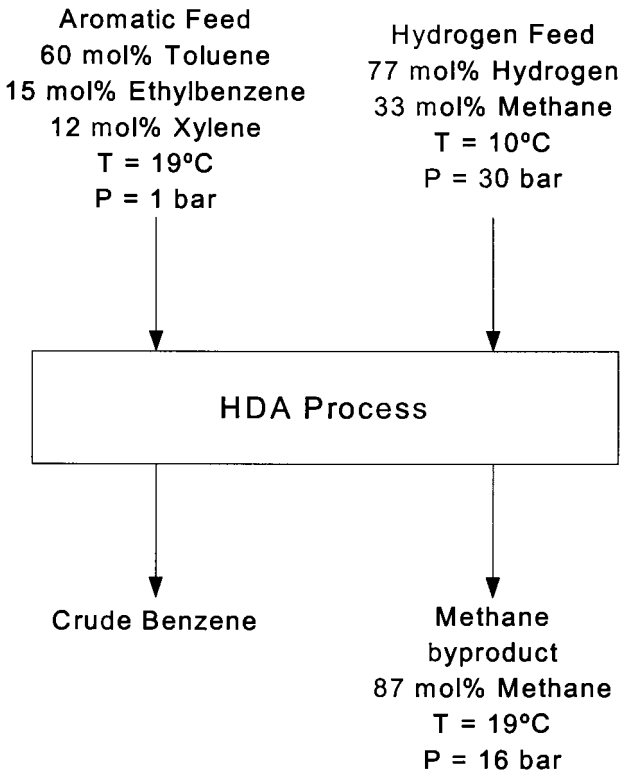

Figure 17: Feed and product streams for the hydrodealkylation simulations

The aromatic feed contains a mixture of alkylaromatic compounds. It is pumped from ambient conditions to the reaction pressure of 60 bar before being heated to 600°C, the reactor inlet temperature.

The hydrogen feed is at a pressure of 30 bar. It mixes with the process' recycle stream before it is compressed to 60 bar and heated to 600°C.

Reactor

Reaction kinetics for the key reactions that occur in the system were obtained from Dow. Due to the confidential nature of this data, it is not conveyed here. This set of reaction kinetics was used with a plug flow reactor model under adiabatic operation.

The reactor dimensions were varied until the overall aromatic conversion reached 95%, the typical conversion for such reactors. The final reactor dimensions were 9m for the tube length and 2.8m for the tube diameter.

Chemoturbine

The discharge pressure was specified as 30 bar. An isentropic efficiency of 75% was suggested based on the properties of the reaction mixture (Ploumen, 2000).

Flash drum feed cooler

The function of this heat exchanger is to cool the expanded reaction mixture before it enters the flash separator. The outlet temperature and pressure specified for this model are 25°C and 30 bar.

Flash drum

The purpose of this unit is to separate the benzene from the other compounds in the reaction mixture.

A sensitivity analysis was performed to determine the optimum flash temperature. The pressure was kept constant at 30 bar. For all temperatures considered, the heavier benzene and aromatic compounds in the reaction mixture were easily removed from the lighter components (hydrogen and methane). Ultimately 25°C was chosen as the best alternative based on the amount of lighter compounds in the crude benzene stream (5 mol%).

At these conditions, the vapour product contains about 34% methane and 61% hydrogen on a molar basis. The high amount of methane in the stream is still a concern: Its presence in the reactor decreases the concentration of the reacting species effectively slowing down the HDA reactions, and, it requires additional compression work. It would be advantageous to remove methane from the recycle loop, preferably prior to the compression step.

Membrane separation

Brinkman (2000) suggested a membrane to avoid the energy intensive cryogenic separation of methane and hydrogen usually employed. Recent studies on the membrane separation of hydrogen and methane revealed that permeation selectivities of 99% are possible with microporous silica membranes (De Vos & Verweij, 1998: 45). These selectivities are moderately dependant on temperature. The optimum temperature for the separation of hydrogen and methane is 200°C.

The membrane was modelled with a black box model due to the lack of an appropriate membrane model in Aspen. The 99% permeation selectivity was specified as the split fraction for hydrogen.

As the flash drum preceding the membrane operates at 25°C, the feed to the membrane is preheated to the optimum separation temperature of 200°C.

Recycle Cooler

The recycle stream was cooled to minimise the compression work requirement. As make-up hydrogen is added to the recycle stream prior to the compression step, it was decided to cool the recycle to the same temperature of the make-up stream. This temperature is 10°C.

Compressor

The combined hydrogen stream (make-up and recycle) is compressed from 30 to 60 bar. An isentropic efficiency of 80% was suggested based on the properties of the working fluid (Ploumen, 2000).

Recycle heater

After compression, the temperature of the combined hydrogen stream has increased to about 90°C, but further heating is required to reach the reactor inlet temperature of 600°C. This heating occurs in the recycle heater.

Methane Expansion Turbine

The methane-rich stream from the membrane separator has a molar purity of 87% making it suitable as a feedstock for downstream processes. As typical conditions for methane feedstocks are 16 bar and 19°C (Luijten, 2000), another opportunity for power production presented itself: the methane-rich stream from the membrane, still at 33 bar and 200°C, was expanded to 16 bar. An isentropic efficiency of 80% was specified (Ploumen, 2000).

Methane cooler

With the expansion of the methane stream, the temperature drops to about 155°C. This stream is then further cooled in a heat exchanger to 19°C.

Compared to typical process values provided by Luijten (2000), the performance of the process shown in Figure 16 is disappointing both in terms of benzene and power production. Additional simulations were performed in an attempt to improve its performance. These are discussed in the next section.

5.4 Flowsheet Improvement and Sensitivity Analysis

5.4.1 Reducing the Reactor Residence Time

The insertion of the membrane separator for the removal of methane created a new difficulty: the 23 mol% methane, usually present in the recycle stream, has now been removed. Hence, the total flow rate of the recycle is a mere 17 kg/h. This reduction in the recycle flow rate causes the reactor's residence time to increase to 150 seconds.

With such a large residence time, the aromatic components spend enough time in the reactor to form heavy aromatic compounds such as the ones given by reactions 19 through 22. The majority of these reactions are endothermic and absorb reaction heat from the exothermic reactions. Besides leaving a smaller amount of heat to convert to power, the presence of heavy aromatic by-products means lower selectivities to benzene and added complexity in downstream separation processes.

Three alternatives were investigated to reduce the residence time:

- Increasing the flow rate of the recycle stream by adding a bypass around the membrane
- Increasing the flow rate of the hydrogen make-up stream
- Reducing the reactor length (volume)

These are discussed next.

1. Adding a bypass around the membrane

The proposed bypass around the membrane separator is shown in Figure 16 with dashed lines. By bypassing the membrane separator the amount of methane in the system will increase. As mentioned previously, this causes a compression work penalty and lower reaction rates. In spite of the negative aspects, this alternative does seem viable as typical recycle streams contain up to 23 mole percent methane (Luijten, 2000).

With the hydrogen make-up flow rate maintained at 2 000 kg/h, the bypass fraction was varied from 0 to 0.8 in steps sizes of 0.2. The results are shown in Figure 18 through Figure 20.

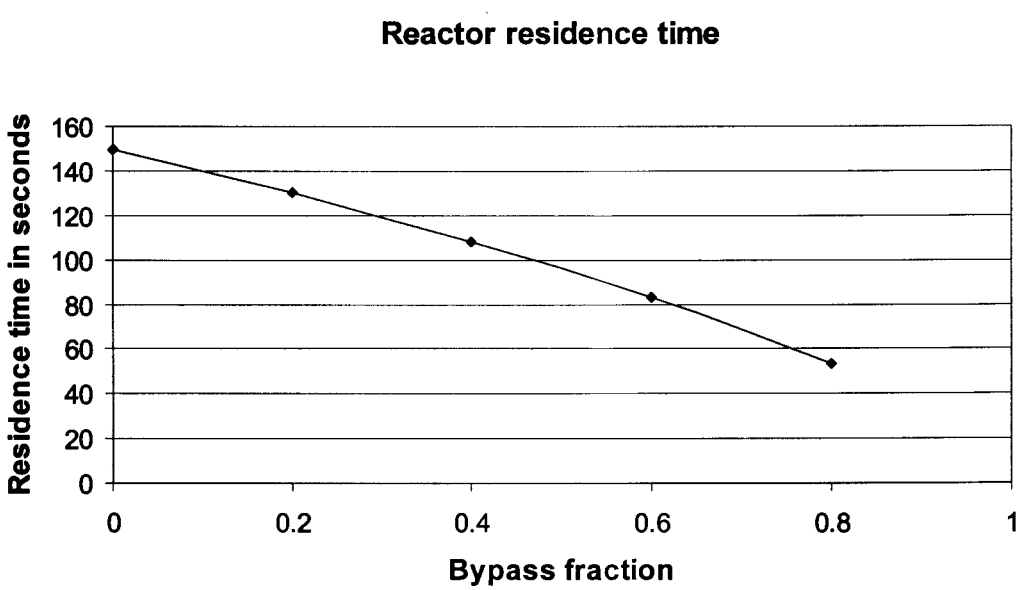

Figure 18: Residence time as a function of the membrane bypass fraction

Figure 18 shows that an increase in the bypass fraction has a significant impact on the residence time in the reactor. One can expect a decrease of between 20 and 25 seconds in the residence time for each increase of 0.2 in the bypass fraction.

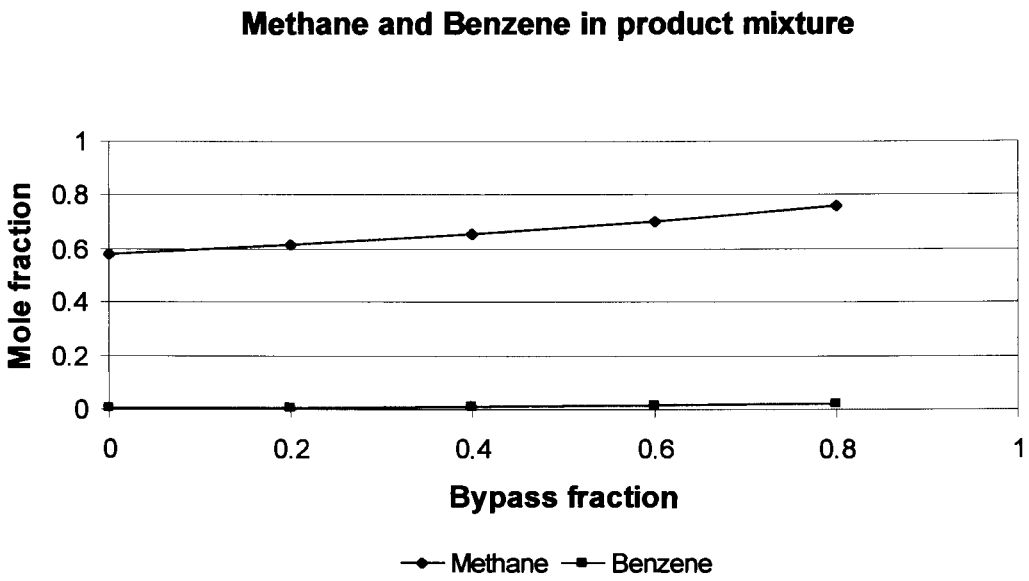

Figure 19: Reactor product mole fractions as a function of the membrane bypass fraction

Figure 19 looks less promising: the benzene in the reactor product is significantly less than the methane over the entire range of bypass fractions.

Figure 20 confirms that this alternative holds little promise. The reactor outlet temperature decreases with each increase in bypass fraction (i.e. with each decrease in residence time). This is due to the large quantities of methane in the reaction mixture. The methane dilutes the reactants causing lower reaction rates and lower reactor outlet temperatures. The power generated by the chemoturbine will be lower as a result of the lower reactor outlet temperatures.

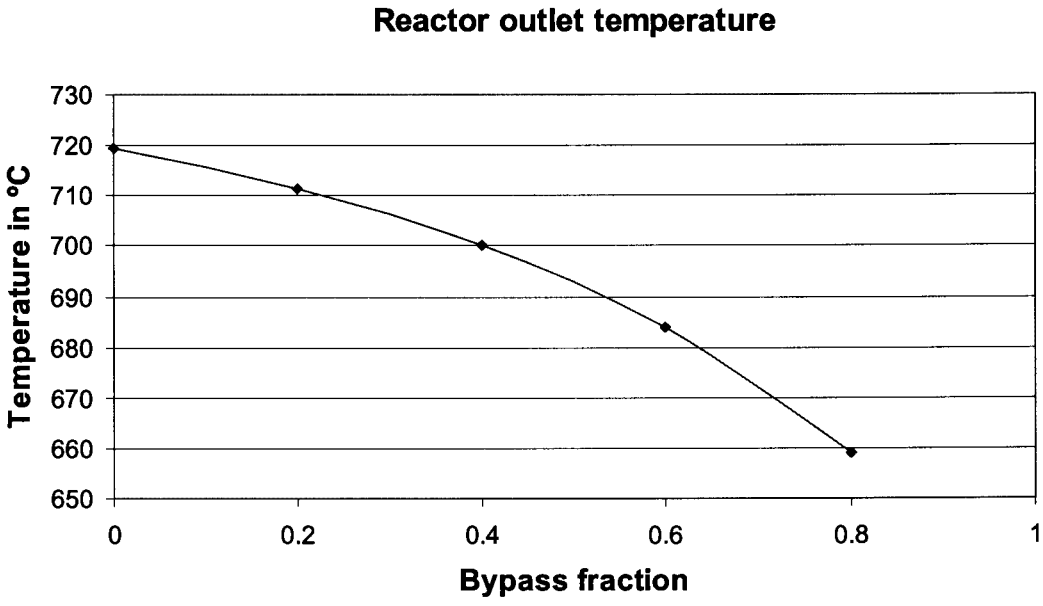

Figure 20: Reactor outlet temperature as a function of bypass fraction

2. Increasing the hydrogen make-up flow rate

With an increase in the hydrogen make-up flow rate, the amount of material passing through the reactor increases and the residence time decreases. The hydrogen make-up flow rate was increased from the typical value of 2 000 kg/h to 6 000 kg/h in step sizes of 1 000 kg/h. The results are shown in Figure 21 and Figure 22.

Figure 21 shows how an increase in the make-up stream's flow rate can decrease the residence time. At a flow rate of 6 000 kg/h the residence time is 39 seconds. This is in close agreement with typical plant values (Luijten, 2000).

Figure 22 shows the changes in the reactor product composition with increasing make-up flow rates. Methane production increases to a maximum at a make-up flow rate of 4 000 kg/h and then declines rapidly. Benzene also appeared to have a maximum production rate for a make-up flow between 5 000 and 6 000 kg/h. The step size was decreased to 250 kg/h and a maximum was observed at a make-up flow rate of 5 500 kg/h. In spite of the maximum benzene production rate, a high amount of methane is also present at 5 500kg/h.

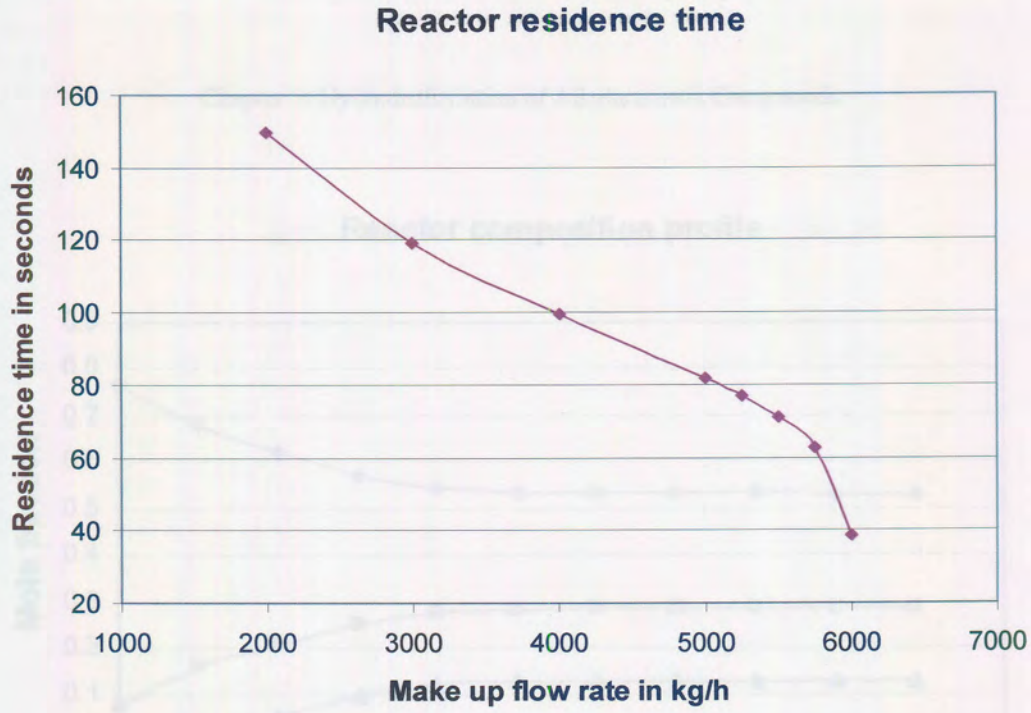

Figure 21: Residence time as a function of make-up flow rate

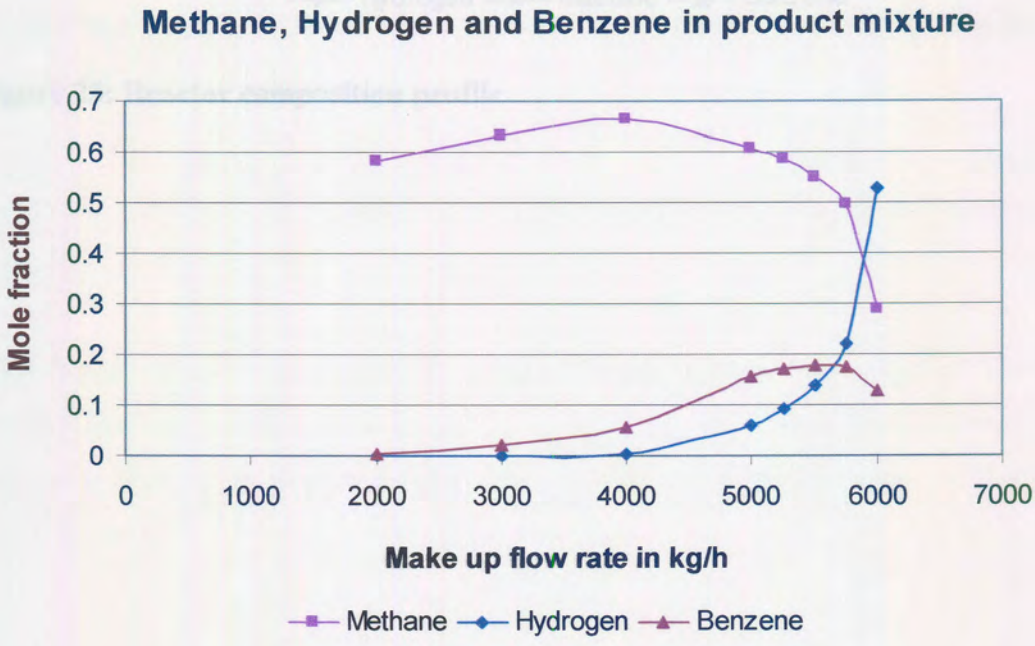

Figure 22: Reactor product mole fraction as a function of make-up flow rate

At the slightly higher make-up flow rate of 6 000 kg/h, the benzene production is only four percent lower than the maximum reached at 5 500 kg/h, but comparatively, the amount of methane is 25% lower than the value observed at 5 500 kg/h. With the high hydrogen-methane separation efficiency of the membrane, only a minute amount of hydrogen is lost through separation and hence the high amount of hydrogen present at this condition does not pose a great concern.

At 6 000 kg/h the reaction outlet temperature is 770°C which is slightly higher than the norm of 730°C. This higher temperature is however welcomed as it would increase the power production in the chemoturbine. Hence, the residence time problem can be solved by increasing the make-up hydrogen flow rate to a value of 6000 kg/h.

3. Reducing the reactor length

By reducing the reactor length, the volume of the reactor is decreased resulting in shorter residence times. Such a reduction can affect reactant conversion and hence the decision can only be made once the effect on conversion has been determined.

Figure 23 depicts the changes in mole fraction of the major species in the reactor (hydrogen, methane and benzene) as a function of reactor length. It is for the specific case of a hydrogen make-up flow rate of 6 000 kg/h, as just described.

The results indicate that the conversion increases and reaches a maximum at a length of 5.4 meters. This corresponds to a benzene mole fraction of 0.13. Beyond this length, no change in composition occurs indicating that the reactor operates at equilibrium conditions. Consequently the reactor length can be shortened from 9m to 5.4m. This would reduce the residence time to 24 seconds.

The final solution to the residence time problem is therefore a combination of alternatives: an increase in the hydrogen make-up flow rate to 6 000 kg/h and a reduction of the reactor length to 5.4 m. These changes are reflected in the flowsheet shown in Figure 24.

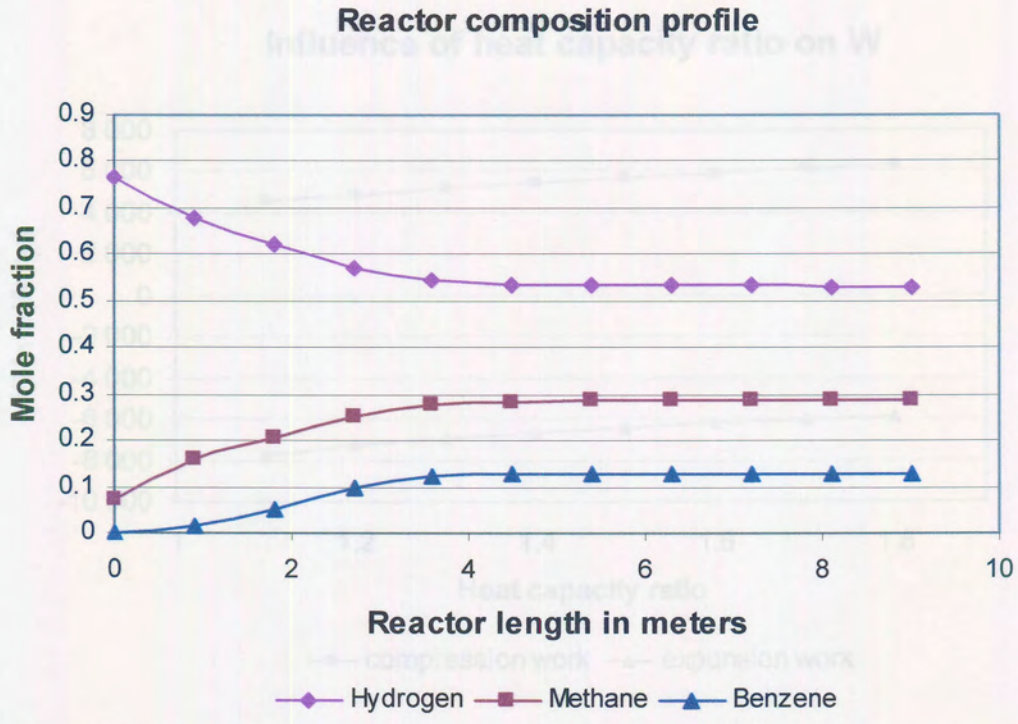

Figure 23: Reactor composition profile

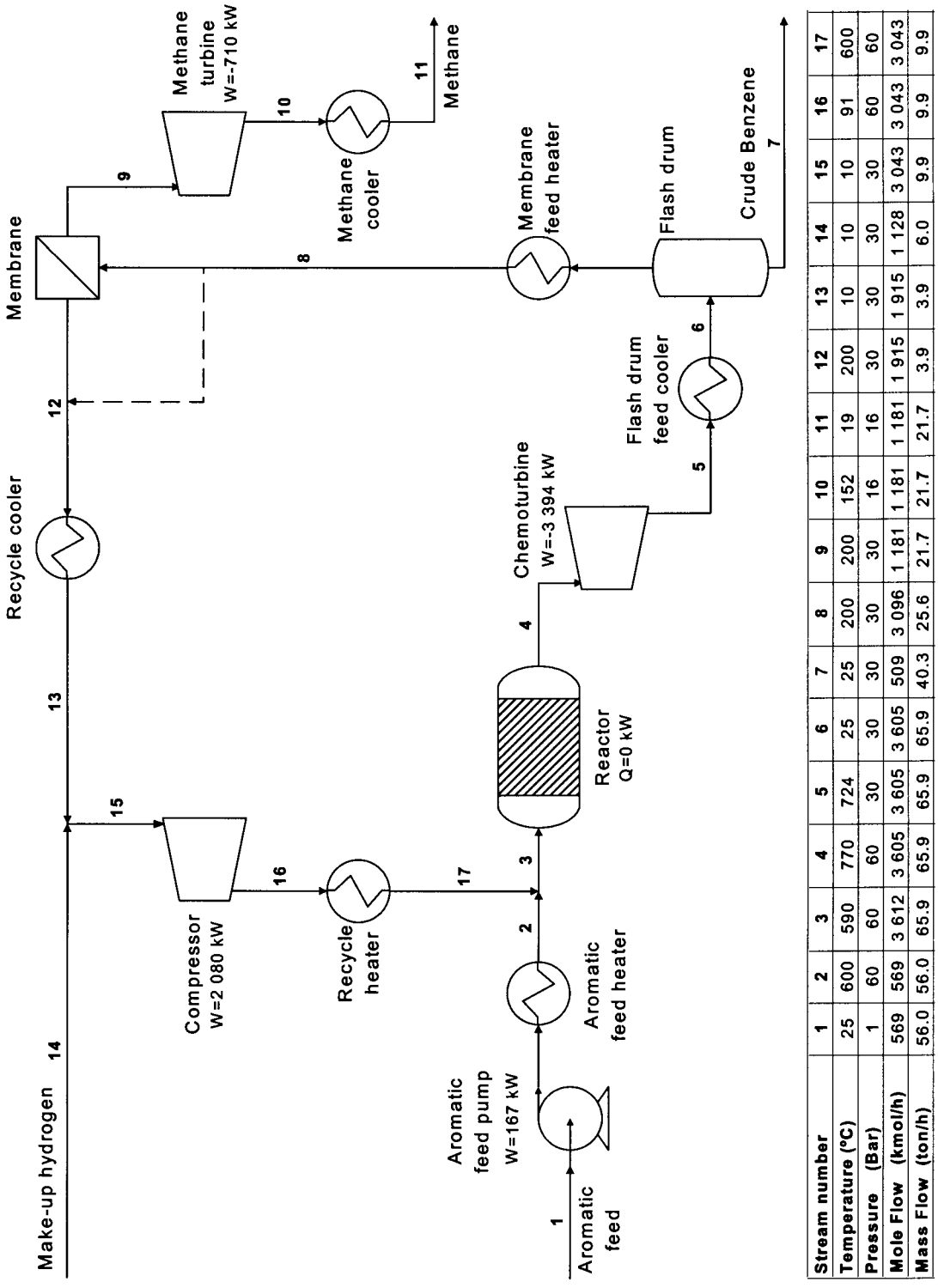

Stream number	1	2	3	4	5	6	7	8	9	10	11	12	13	14	15	16	17
Temperature (°C)	25	600	590	770	724	25	25	200	200	152	19	200	10	10	10	91	600
Pressure (Bar)	1	60	60	60	30	30	30	30	30	16	16	30	30	30	30	60	60
Mole Flow (kmol/h)	569	569	3 612	3 605	3 605	3 605	509	3 096	1 181	1 181	1 181	1 915	1 915	1 128	3 043	3 043	3 043
Mass Flow (ton/h)	56.0	56.0	65.9	65.9	65.9	65.9	40.3	25.6	21.7	21.7	21.7	3.9	3.9	6.0	9.9	9.9	9.9

Figure 24: Updated flowsheet for the hydrodealkylation process as simulated in Aspen Plus

5.4.2 Sensitivity Analysis to Increase Power Production

It is shown in Appendix B that the heat capacity ratio (κ) has a significant impact on the amount of power required and gained during compression and expansion. In both cases, lower κ-values are more favourable.

It was observed that streams with high average molecular weights (i.e. containing more aromatic compounds) have lower κ-values than streams with low molecular weights (i.e. streams containing more hydrogen, methane and ethane).

To increase the net power production from the system shown in Figure 24, a method was sought to lower the κ-values of the compressor and chemoturbine feeds. Since the hydrogen make-up stream affects both the compressor and chemoturbine feeds, it was again selected as the manipulated variable.

The make-up flow rate was lowered from 6 000 kg/h to 5 750 kg/h. The reasoning behind this reduction is explained by referring back to Figure 22. At 5 750 kg/h, the reaction product mixture (chemoturbine feed) contains four percent more benzene while the sum of the hydrogen and methane fraction is ten percent lower than that at 6 000 kg/h. With the reduction in the κ-value of the chemoturbine expected to be larger than that of the compressor, the net power production for these two units (and for the process as a whole) should also increase.

The results of this sensitivity analysis are shown in Table 9.

As expected, the κ-value of the chemoturbine feed decreased by 3.5% when the make-up hydrogen flow rate was decreased. The compressor feed κ-value remained unchanged.

Table 9: Influence of the hydrogen make-up flow rates on the heat capacity ratio and power production

Parameter	Make-up flow rate in kg/h	
	5 750	6 000
Compressor		
Mole flow (kmol/h)	1 550	3 040
Mole Fraction		
Hydrogen	0.84	0.91
Methane	0.16	0.09
κ-value	1.40	1.40
Temperature increase over compressor (°C)	80	81
Compressor power (kW)	-1 060	-2 080
Chemoturbine		
Mole flow (kmol/h)	2 110	3 605
Mole Fraction		
Hydrogen	0.22	0.53
Methane	0.50	0.29
Benzene	0.18	0.13
κ-value	1.09	1.13
Temperature decrease over chemoturbine (°C)	33	46
Chemoturbine power (kW)	2 080	3 395
Chemoturbine – compressor power (kW)	1 020	1 315

The difference between the chemoturbine and compressor power values did not increase as predicted, but decreased. This decrease is attributed to the smaller flow rates through the compressor and chemoturbine (down by 49 and 41% respectively) and the 13°C lower temperature drop over the chemoturbine at the smaller flow rate. Consequently, the case shown in Figure 24 still takes preference.

5.4.3 Summary of the Improved Flowsheet Parameters

The key parameters for the improved, final flowsheet, as shown in Figure 24, are summarised in Table 10.

Table 10: Parameters for the improved flowsheet

Parameter	Value	Units
Feedstocks		
Aromatic feed flow rate	56 000	kg/h
Make up flow rate	6 000	kg/h
Reactor		
Reactor length	5.4	m
Residence time	24	s
Reactor outlet temperature	770	°C
Reactor product flow rate	65 890	kg/h
Component flow in reactor product		
Hydrogen	3 820	kg/h
Methane	16 720	kg/h
Ethane	4 320	kg/h
Benzene	36 400	kg/h
Heavy aromatic compounds	4 470	kg/h
Chemical Products		
Crude Benzene at 89 mol% purity	40 300	kg/h
Methane at 87 mol% purity	21 700	kg/h
Power production		
Total compression power (MW)	2.25	MW
Total expansion power (MW)	4.10	MW
Net power production (MW)	1.85	MW

Although a threefold increase in hydrogen make-up is required, the 56 000 kg/h aromatic feed is hydrodealkylated to 36 400 kg/h benzene, in close agreement with typical values. The make-up increase is necessary to compensate for the removal of high purity methane. The latter is suitable for feedstock use in a downstream chemical process.

Other consequences of the enlarged make-up stream include a reduction in the reactor length and an increase in the reactor outlet temperature.

The total power requirement of the plant (aromatic feed pump and compressor) amounts to 2.25 MW. This is less than the 4.1 MW produced by the chemoturbine and methane expansion turbine and, as a result, 1.85 MW is available for export to other processes.

5.5 Conclusions

This case study focused on the conceptual design of a flowsheet that includes a chemoturbine directly behind the reactor. The chemoturbine is responsible for all of the reaction heat recovery as the reactor is operated adiabatically.

A membrane separator was employed rather than the typical cryogenic separation to obtain a high purity hydrogen recycle. By doing so, a methane by-product stream of high purity became available for downstream use, but the reactor performance deteriorated due to a smaller recycle flow rate.

Results from subsequent simulations, aimed at improving the flowsheet, showed that the process performance could be restored to typical values by increasing the flow rate of the hydrogen make-up to 6 000 kg/h. The reactor length can also be shortened to 5.4 m. With these changes, the benzene production rate will be 40 300 kg/h and 1.85 MW of power can be exported from the process.

Chapter 6: Conclusions and Recommendations

Three chemical processes, namely ethylene oxide production, phthalic anhydride production as well as the hydrodealkylation of alkylaromatic compounds, were studied to determine the feasibility of chemoturbine integration into chemical processes. The intended function of the chemoturbine is to convert reaction heat to mechanical or electrical power.

Among others, there are two significant differences between the three processes that influenced the flowsheet development. The first difference is the reactor operating conditions. Heat is removed from the phthalic anhydride reactor (isothermal operation) whilst the hydrodealkylation reactor has no heat removal (adiabatic operation). The ethylene oxide reactor has heat removal and a temperature increase towards the reactor outlet and hence, contains aspects characteristic to both isothermal and adiabatic reactors.

Heat removal from the reactor has a significant impact on the amount of power that can be obtained from the chemoturbine. The amount of reaction heat available for recovery by a chemoturbine decreases when heat is removed from the reactor. The phthalic anhydride process is an example of a case where heat removal was necessary. Here the chemoturbine only played a secondary role in power production. The majority of the power is produced by the steam turbine.

The second difference between the case studies is in the conversions achieved in the reactor. Low reaction conversions necessitate recycle streams. Recycle streams are employed in both the ethylene oxide and hydrodealkylation case studies. The presence of a recycle stream means that additional separation devices are necessary and the recycle stream has to be recompressed to the reaction pressure.

Along with the mentioned differences there are similarities in the simulation results of the three processes. Results show that power has to be supplied to the conventional processes without chemoturbines. With the addition of chemoturbines the full power requirements of each process could be fulfilled and excess power was available for

export. Hence, it is feasible to incorporate chemoturbine units in the three processes considered.

When a chemoturbine is integrated into a chemical process it may be necessary to alter operating conditions of some process units from their normal values. Since the process now has an additional product namely power, a re-evaluation of all the operating conditions and tradeoffs in the process is necessary. Further investigation on the impact of chemoturbine integration on the optimal operating conditions of the process is therefore recommended.

Comparing processes where power is imported under certain conditions and exported under other conditions are difficult, because traditional efficiency definitions usually apply to only one of these situations. The thermal conversion efficiency used in the phthalic anhydride case does not include feed compression power. Hence, its use is limited to the evaluation of the energy conversion from a high temperature heat source to power. For a more comprehensive evaluation of the process performance, all of the power terms should be represented in the efficiency definition. It is therefore recommended that a new parameter be formulated to characterise the performance for processes of this nature.

When formulating a new parameter for evaluating processes that co-produce power and chemicals, it should be kept in mind that, in some systems temperature increases are beneficial to both chemical product and power production. It might appear feasible to rate the performance of the system as the ratio of power generated to the amount of chemical product synthesised. However, if the chemical production decreases and the power production increases at higher temperatures, a performance indicator based on the mentioned ratio will give erroneous results (i.e. power production will increase and amount of product will decrease giving a higher performance indication).

The usefulness of exergy analysis was illustrated in the phthalic anhydride case. It provides insight as to where the greatest thermodynamic losses occur in a process. The isenthalpic expansion valve was the third largest source of exergy loss in the phthalic anhydride process. An increase of 4.5% in the process' degree of perfection

was observed when it was replaced by a chemoturbine. Similar analyses should also be performed for the two remaining cases to assess their degree of perfection.

The integration of power cycles and chemical processes is truly of a multidisciplinary nature. It requires expertise of several different fields including process synthesis, chemical unit operations, power generation, simulation as well as thermodynamics (exergy analysis). A team consisting of process design engineers, power engineers and thermodynamic specialists are ideally required in the development and design stages of such a process.

Reference List

AspenTech (1999) *Aspen Plus Version 10. Physical Property Methods and Models*, Aspen Technology Inc.

Austin, G.T.. (1984) *Shreve's Chemical Process Industries, Fifth Edition*, McGraw-Hill, New York.

Barber, E.M., Muenger, J.R., Alexander, D.L. (1981) "Combination chemical plant and Brayton-cycle power plant", *US Patent 4,273,743*, assigned to Texaco Inc, US.

Bram, S. and De Ruyck, J. (1997) "Exergy analysis tools for Aspen applied to evaporative cycle design", in *Energy Conversion and Management, 38* (15-17), 1613-1624.

Brinkman, E. W. (2000) *Personal communication*. Doctor in Engineering, Ceramic Technology (Materials Division), Netherlands Organisation for Applied Scientific Research, Email address: brinkman@tpd.tno.nl

Coombs, J., Kim D. and Palombo L. (1997) "Celanese Clearlake ethylene oxide reactor revamp", http://www.owlnet.rice.edu/~ceng403/ethox97.html, accessed 15 August 2001.

Cunningham, J. W., Foster, E. G., and Vanderwater, R. G. (1971) "Secondary removal of inerts in ethylene oxide purification", US Patent 3,766,714, assigned to Shell Oil Company, US.

Deutner W. and Neumann R. (1975) "Process for the preparation of pure phthalic anhydride", *US Patent 3 886 050*, assigned to Chemie Linz AG, Austria.

Dever, J. P., George, K. F., Hoffman, W. C. and Soo, H. (1995) "Ethylene oxide" in *Kirk Othmer Encyclopaedia of Chemical Technology, 4th Edition*, Vol. 9, 915-959, Kroschwitz, J. I. (executive editor), John Wiley and Sons, New York, US.

De Vos, R. M. and Verweij, H. (1998) "Improved performance of silica membranes for gas separation" *Journal of Membrane Science, 143*, (1-2), 37-51.

Dijkema, G.P.J., Luteijn, C.P. and Weijnen, M.P.C. (1998) "Design of trigeneration systems", in *Chemical Engineering Communications, 168*, 111-125.

Doldersdum, A. (1998) *Exercom (Version 2) Manual for Aspen Plus Version 10 (PC-Version), Volume 1: Enthalpy and Exergy Function for Gases and Liquids*, Stork Engineers and Contractors B.V., Amsterdam, The Netherlands.

Greeff I. L., Ptasinski K. J. and Janssen, F. J. J. G. (2001) "Integration of a turbine expander with an exothermic reactor for the combined production of power and ammonia", in *Proceedings of ECOS 2001, 1*, 369-375, Öztürk, A. and Göü, Y.A. (editors), Istanbul, Turkey.

Harvey, S. and Kane, N. (1997) "Analysis of a reheat gas turbine cycle with chemical recuperation using Aspen" in *Energy Conversion Management, 38*, (15-17), 1671-1679.

Herdillia Chemicals Limited, product specification website, "Phthalic anhydride" http://www.herdillia.com/htm/phthalic.htm. Accessed on 27 July, 2001.

Hinderink, A.P., Kerkhof, F.P.J.M., Lie, A.B.K., De Swaan Arons, J. and van der Kooi, H.J. (1996) "Exergy analysis with a flowsheeting simulator-I. Theory; calculating exergies of material streams" in *Chemical Engineering Science, 51* (20), 4693-4700.

Horton, A. (1969) "Process and apparatus for the manufacture of nitric acid", *GB Patent 1,146,292*, assigned to Humphreys and Glasgow Limited, UK.

Janssen, F. J. J. G., Verkooijen, A. H. M. and Ploumen, P.J. (1997) "Synthesis of ethene", *European Patent 0,753,652*, assigned to Kema NV, the Netherlands.

Kotas, T.J. (1995) *The Exergy Method of Thermal Plant Analysis*, Krieger Publishing, Malabar, Florida, US.

Kunii, D. and Levenspiel, O. (1991) *Fluidization Engineering, Second Edition*, Butterworth-Heinemann, Boston, US.

Linnhoff, B., Le Leur, J. E. and Pretty, B. L. (1988) "Exothermal chemical reaction processes", *European Patent 0,301,844 B1*, assigned to British Technology Group Limited, UK.

Lorz, P. M., Towae, F. K., Enke, W., Jäckh, R. and Bhargava, N. (2001) "Phthalic acid and derivatives - Phthalic Anhydride" in *Ullmann's Encyclopedia of Industrial Chemistry Online*, http://jws-edck.interscience.wiley.com, Accessed 26 June 2001.

Luijten, S.J. (2000) *Personal communication*. Process engineering specialist, Energy Process Development & Control Department, Dow Chemicals Benelux N.V. Email address: sjluijten@dow.com

Mistry, A. S., King, S. M. and Paxton, C. S. (1997) "Ethylene oxide separation design" http://www.owlnet.rice.edu/~ceng403/gr2699/armadillo.html, accessed 15 August 2001.

Ozero, B. J. and Landau, R. (1984) "Ethylene oxide" in *Encyclopedia of Chemical Processing and Design - 20, Ethanol as fuel; options, advantages and disadvantages to exhaust stacks, cost*, McKetta, J. J. (executive editor), Dekker Publishing, New York, US.

Ploumen, P.J. (2000) *Personal communication*. Doctor in Engineering. Power Generation and Sustainables Group, Kema Nederland B.V. Email address: p.j.ploumen@kema.nl

Prokopiev, S. I., Aristovm Y.I. and Parmon, V. N. (1997) "Zero-emission turbine on the basis of reversible monofuels as a tool for ecologically sound power engineering:

thermodynamic analysis of new flow diagram", *International Journal for Hydrogen Energy, 22* (4) 415-421.

Rebsdat, S. and Mayer, D. (1991) "Ethylene oxide", in *Ullman's Encyclopaedia of Industrial Chemistry*, A10, 117-126, Gerhartz, W (Executive Editor), VCR Vertrieb Publishers, Dsseldorf, Germany.

Rosen, M.A. (1996) "Thermodynamic comparison of hydrogen production processes", in *International Journal of Hydrogen Energy*, *21* (5), 349-365.

Ryder, R. C., Ryan, R. E. and Klapproth, W. J. (1974) "Process for the production of phthalic anhydride", *US Patent 3 852 308,* assigned to Koppers Company, US.

Scharpf, E. W. and Sorensen J. C. (1997) "Gasification combined cycle power generation process with heat-integrated chemical production", *US Patent 5,666,800*, assigned to Air Products and Chemicals, US.

Sorin, M., Lambert, J. and Paris, J. (1998) "Exergy flows analysis in chemical reactors", in *Transactions of the Institute of Chemical Engineers*, *76*, (A), 389-395.

Stahl, C. R. (1983) "Combined cycle apparatus for synthesis gas production", *GB Patent 2,111,602 A*, assigned to General Electric Company, US.

Szargut, J., Morris, D.R, Steward, F.R. (1988) *Exergy Analysis of Thermal, Chemical and Metallurgical Processes,* Hemisphere Publishing, New York, US.

Tsatsaronis G. (1999) "Strengths and limitations of exergy analysis", in *Thermodynamic optimization of complex energy systems,* Bejan A. and Mamut, E., (editors), 93-100.

Underwood, J. Dawson, G. and Barney, C. (1997) "Design of a CO_2 absorption system in an ammonia plant" http://www.owlnet.rice.edu/~ceng403/co2abs.html, accessed 15 August 2001.

Wainwright, M. S. and Foster, N. R. (1979) "Catalysts, kinetics and reactor design in phthalic anhydride synthesis" in *Catalysis Reviews. Science and Engineering*, *19* (2), 211-292.

Westerterp, K. R. and Ptasinski, K. J. (1984) "Safe design of cooled tubular reactors for exothermic, multiple reactions; parallel reactions-II The design and operation of an ethylene oxide reactor" in *Chemical Engineering Science*, *39*, (2) 245-252.

Winnick, J. (1997) *Chemical Engineering Thermodynamics*, John Wiley and Sons, New York, US.

Appendix A: Terms in the Exergy Balance

Before discussing each term in the exergy balance, it is important to note that exergy calculations are always evaluated between the process conditions and one of two equilibrium states (similar to the reference state in the energy balance). These states are known as restricted and unrestricted equilibrium. In restricted equilibrium, (commonly referred to as the environmental state) the pressures and temperatures of the system and the environment are equal but chemical equilibrium has not been reached. This means that there are no pressure or temperature driving forces between the system and the environment that have the potential to do work. Chemical potential differences between the system and the environment still exist and hence there is a driving force capable of further work production. In unrestricted equilibrium (or dead state), chemical equilibrium also exists and the chemical potential difference is zero.

Each term in the exergy balance is discussed in the following paragraphs.

Exergy associated with work transfer ($\dot{W}$): Through its definition, exergy is equivalent to work in every respect (Kotas, 1995: 34), hence this term has the exact numerical value as in the energy balance. The sign convention used in this investigation defines work transferred from the environment to the system as positive.

Exergy associated with heat transfer ($\dot{E}^{Q}$): This is the exergy obtainable from the conversion of heat (Q) to work. Heat transfer exergy is mathematically given by:

$$\dot{E}^{Q} = Q\tau \qquad \text{(A1)}$$

and

$$\tau = 1 - \frac{T_0}{T_r} \qquad \text{(A2)}$$

with T_0 the temperature of the environment and T_r, the temperature at the system boundary where the heat transfer takes place (Kotas, 1995: 34). In this investigation, heat transfer to the system has a positive sign.

Exergy associated with material flow ($\dot{E}$): when nuclear, magnetic, electric and surface tension effects are neglected, this exergy is subdivided in kinetic (ε_k), potential (ε_p), physical (ε_{ph}) and chemical exergy (ε_0). The components are added to obtain the total exergy of a material stream:

$$\dot{E} = \dot{m}\left(\varepsilon_k + \varepsilon_p + \varepsilon_{ph} + \varepsilon_0\right) \tag{A3}$$

The kinetic and potential exergy components are ordered forms of energy and thus fully convertible to work. They are equal to the kinetic and potential energy terms in the energy balance. As in the energy balance, their contribution to the total exergy of material streams are usually negligible.

Physical and chemical exergy are both forms of disordered energy and have to be evaluated relative to a predefined state.

Physical Exergy (ε_{ph}): is the maximum work obtainable when moving the system from its initial condition to the environmental state using physical processes which involves only thermal interaction between the system and the environment (Kotas, 1995: 38). It is given by:

$$\varepsilon_{ph} = (h_1 - T_0 s_1) - (h_0 - T_0 s_0) \tag{A4}$$

Physical exergy can also be subdivided in temperature and pressure change components:

$$\varepsilon_{ph}^{\Delta T} = \left[- \int_{T_1}^{T_0} \frac{T - T_0}{T} dh \right]_{P_1} \tag{A5}$$

and

$$\varepsilon_{ph}^{\Delta P} = T_0(s_0 - s_1) - (h_0 - h_1) \qquad \text{(A6)}$$

that can be calculated individually, attributed to it being evaluated between two thermodynamic states (0 and 1).

Chemical Exergy (ε_0): is the maximum work obtainable when a substance is brought from the environmental state to the dead state by processes involving heat transfer and exchange of substances with the environment alone. In other words, this is the work potential of a substance attributed to the difference in the chemical potentials of the substance and that of a reference substance in environment. When utilising the concept of standard chemical exergy (Szargut *et al.*, 1988: 56), the chemical exergy of a material stream can be calculated with the formula:

$$\varepsilon_0 = \sum x_i \varepsilon_i^0 + RT_0 \sum_i x_i \ln \gamma_i x_i \qquad \text{(A7)}$$

with

x	mole fraction
ε^0	standard chemical exergy in kJ/kmol
R	universal gas constant in kJ/kmol K
T_0	environmental temperature in K
γ	activity coefficient

Appendix B: Pressure Changer Principles

The governing equations for the adiabatic, reversible pressure change of an ideal gas are briefly reviewed. For more information and detailed derivations of equations, consult a textbook on Thermodynamics such as Winnick (1997: 144-147). A compressor is used as an example, but the equations are equally applicable to turbine expanders.

Figure B1 shows a compressor with inlet conditions (1) and outlet conditions (2).

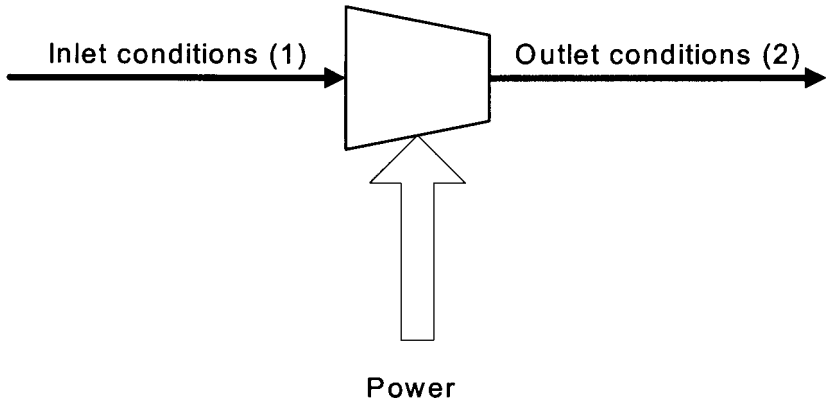

Figure B1: Compressor with fluid flow and power supply

Potential and kinetic energy differences are negligible and since these machines operate adiabatically, the energy balance reduces to (Winnick, 1997: 144):

$$W = \Delta h \qquad \text{(B1)}$$

Hence, the work necessary to bring about a pressure change is the difference between the outlet and inlet enthalpies of the working fluid. Under the assumption of an ideal gas with constant heat capacity, the work can also be written as a function of inlet temperature, pressure ratio and heat capacity ratio (Winnick, 1997: 146):

$$W = RT_1\left(\frac{\kappa}{\kappa-1}\right)\left[\left(\frac{P_2}{P_1}\right)^{\left(\frac{\kappa-1}{\kappa}\right)}-1\right] \qquad \text{(B2)}$$

where

R	universal gas constant (kJ/kmol.K)
T_1	inlet temperature (K)
P_1	inlet pressure (bar)
P_2	outlet pressure (bar)
κ	heat capacity ratio

The heat capacity ratio is given by

$$\kappa = \frac{C_P}{C_v} \qquad \text{(B3)}$$

with

C_P	heat capacity at constant pressure (kJ/kmol.K)
C_v	heat capacity at constant volume (kJ/kmol.K)

From equation B2, one can see that the amount of work required to compress a gas increases when the inlet temperature or pressure ratio increases. Conversely, for expanders, more work can be obtained at high inlet temperatures and pressure ratios.

The effect of the heat capacity ratio on the work required by a compressor is obscured by its multiple occurrences in the formula, but the graphical representation of equation B2, illustrated in Figure B2, shows its influence.

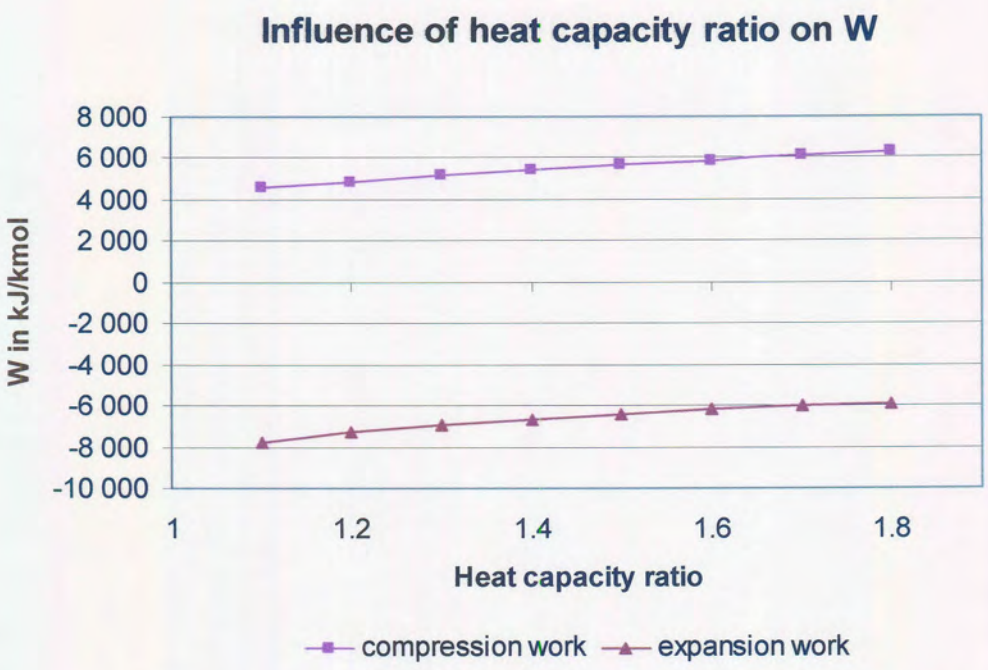

Figure B2: Influence of the heat capacity ratio on the power required for a specified pressure change

Figure B2 reveals that lower heat capacity ratios correspond with lower compression work.

When recalling that power from the system to the environment has a negative sign (by convention) one can see that a similar conclusion can be drawn for expansion processes. More work can be obtained when the fluid to be expanded has a lower heat capacity ratio.

Appendix C: Rankine Power Cycles

A short review of Rankine cycles is presented. Interested readers are referred to thermodynamic textbooks such as Winnick (1997) for more information.

The operations of an isentropic Rankine cycle is superimposed on the temperature-entropy diagram shown in Figure C1.

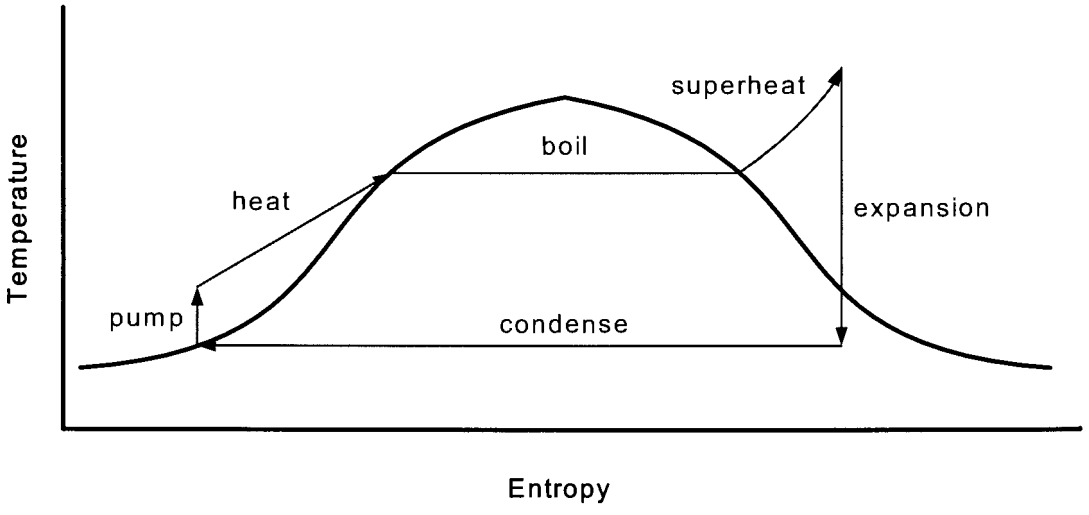

Figure C1: Temperature-entropy diagram of a Rankine cycle

There are two pressure levels in the cycle: the condenser and boiler pressures. The condenser pressure is lower than the boiler pressure.

The cycle starts with the pumping of a working fluid (for example water) in the liquid phase. A pump is used because pumping a liquid does not require as much power as compressing a gas.

At the boiler pressure, the liquid is usually subcooled (below saturation temperature). It is heated, vaporised and superheated by hot combustion gases in a furnace. The three heating steps take place at constant pressure.

The superheated steam enters the steam turbine where it is expanded to the condenser pressure. The physical energy present in the superheated steam is converted to kinetic energy in the expansion process. A two-phase mixture of vapour and liquid exists at the turbine exhaust. This mixture is condensed and the cycle is repeated.

The unit operations in the Rankine cycle are shown in Figure C2.

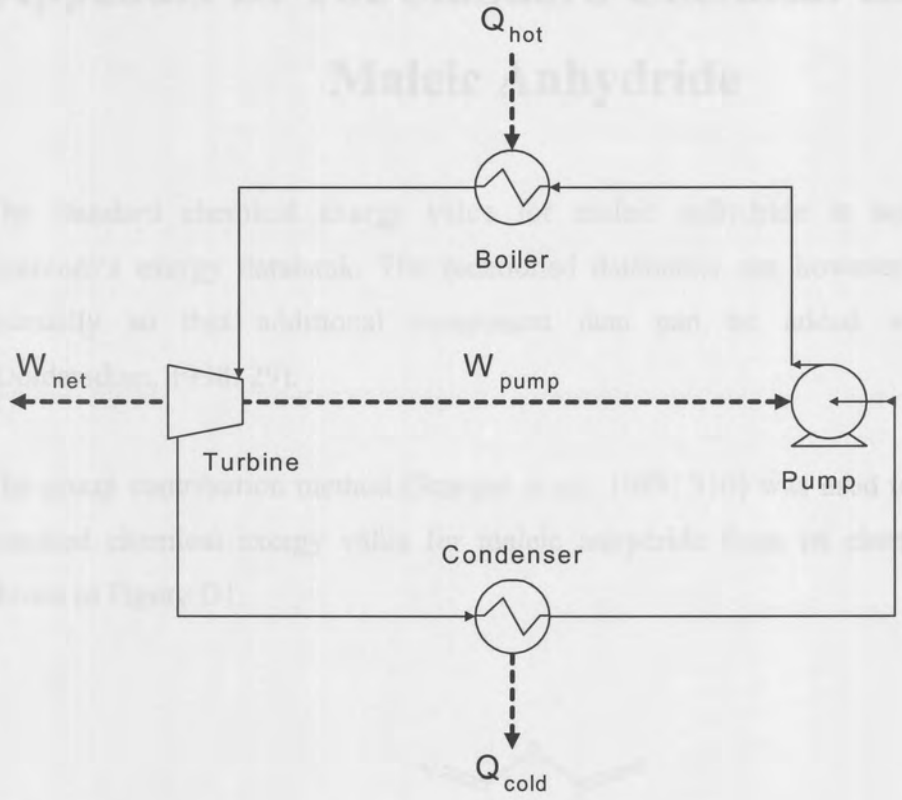

Figure C2: Rankine cycle power plant schematic

Typical operating parameters for Rankine cycles are summarised in Table C1.

Table C1: Summary of typical steam cycle operating parameters

Parameter	Value	Reference
Boiler pressure	180 bar	Austin, 1984: 56
Condenser pressure	0.04 bar	Winnick, 1997: 173
Turbine inlet temperature	540°C	Austin, 1984: 56
Vapour fraction at turbine outlet	min. 90%	Winnick, 1997: 177

Appendix D: The Standard Chemical Exergy of Maleic Anhydride

The standard chemical exergy value for maleic anhydride is not included in Exercom's exergy databank. The mentioned databanks can however be appended manually so that additional component data can be added when required (Doldersdum, 1998: 29).

The group contribution method (Szargut *et al.*, 1988: 310) was used to calculate the standard chemical exergy value for maleic anhydride from its chemical structure shown in Figure D1.

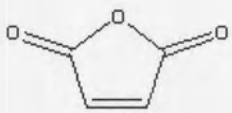

Figure D1: Chemical structure of maleic anhydride

The groups used in the calculations are listed in Table D1.

Table D1: Standard chemical exergies for the groups in maleic anhydride

Group	Number of Occurrences	Standard chemical exergy for gas (kJ/mol)	Standard chemical exergy for liquid (kJ/mol)
—O— (ring)	1	-97.12	-106.64
O ‖ —C— (ring)	2	305.66	277.76
| =CH (ring)	2	576.65	568.28

Therefore

$$\varepsilon^{0}_{\text{Maleic Anhydride}} = -97.12 + 2 \times 305.66 + 2 \times 576.65 = 1667.50 \text{ kJ/mol}$$

for the gaseous phase and

$$\varepsilon^{0}_{\text{Maleic Anhydride}} = -106.64 + 2 \times 277.76 + 2 \times 568.28 = 1585.44 \text{ kJ/mol}$$

for the liquid phase.